FINAL REPORT

NASA Grant NGR-14-005-107

NONLINEAR DYNAMIC ANALYSIS OF STRUCTURES

by

John W. Leonard

Final Report of a Project in Cooperation with

The University of Illinois
Department of Civil Engineering
Urbana, Illinois

and

The National Aeronautics and Space Administration

November 4, 1968

This report summarizes the results of the study of the dynamic response of inflatable shells for the period June 15, 1967 to November 4, 1968.

The equations of motion were derived for an isotropic inflatable shell with a general configuration and a solution procedure was developed to determine the natural frequencies and modes of free vibrations of shells of revolution with arbitrary meridional contours. A computer program to implement this solution procedure was developed and tested on several sample problems.

The forced response of inflatable shells of revolution was studied by means of a modal method of analysis. This general solution technique was tested using the same sample problems used to illustrate the free vibration solution technique.

The detailed results of this project are described in the attached paper, submitted for review by the American Society of Civil Engineers for publication in the Journal of the Engineering Mechanics Division. Reprints of this paper and of a previous paper based in part on the results of this grant will be transmitted when available.

PUBLICATIONS

Leonard, J.W., "Inflatable Shells: Non-Symmetric In-Service Loads," Journal of the Engineering Mechanics Division, ASCE, Vol. 94, No. EM5, Oct. 1968.

Leonard, J.W., "Dynamic Response of Initially-Stressed Membrane Shells," submitted for publication in the Journal of the Engineering Mechanics Division, ASCE.

PERSONNEL

The personnel employed half-time were Dr. John W. Leonard, Assistant Professor of Civil Engineering, and Mr. Tzu-Cheng Chu, Research Assistant in Civil Engineering. The services of Drs. N.M. Newmark, A.R. Robinson, and W.C. Schnobrich were provided by the University of Illinois without charge to the project.

DYNAMIC RESPONSE OF INITIALLY-STRESSED MEMBRANE SHELLS

by John W. Leonard, A.M. ASCE[1]

INTRODUCTION

This study is concerned with the dynamic behavior of extremely thin shells which have attained a given stress state due to previous loads. The response of these structural components to the action of further in-service dynamic loads will be studied and the effects of the initial stress state determined.

Initially-stressed thin shells have of late been used as temporary enclosures at expositions, as prefabricated warehouses and fuel tanks, and as inflatable concrete forms for dome construction. They have been considered for use in the erection of space and lunar structures. For example, certain space structures proposed for Saturn-Apollo applications can be optimized using such components: their in-service structural rigidity being obtained via pressurization. Possible applications in the near future for such light-weight structures include space vehicle antennas and connecting tunnels between stages of manned orbiting stations or lunar modules.

An important aspect of the behavior of initially-stressed thin shells is their action under in-service dynamic loads. For example, the behavior of an inflated satellite is influenced by the dynamic nature of the inflation process in that the shell arrives at its desired final configuration with a finite velocity field. It is also influenced by control forces, external forces such as gravity and solar pressures, and forces caused by movement of personnel

---

[1]Assistant Professor of Engineering and Applied Science, State University of New York at Buffalo, Buffalo, New York.

and propellant. Two other dynamics problems are 1) the effect on inflated concrete forms of the large impact forces which result when shotcrete is applied, and 2) the effect of winds and earth tremors on shells used as temporary shelters, warehouses, and fuel tanks.

The behavior of extremely thin initially-stressed membrane shells is such that classical methods are inadequate for their proper analysis. In recent years considerable attention has been given to the derivation of consistent shell theories (2, 16, 23, 28, 32)[2] and to the development of solutions for nonlinear membrane shell problems (6, 10, 14, 18, 29). Another area of recent research is the representation of nonlinear problems as a sequence of superpositions of linear problems, static and dynamic, on previously solved linear or nonlinear problems, e.g. prestressed membranes (1, 19, 20, 22). The classical dynamic behavior of thin shells of revolutions has been studied, and solution methods for the symmetric and asymmetric modes of free vibrations have been presented (3, 8, 11, 22, 24, 26, 27, 31).

In the following study, the equations of motion for a thin shell with a general configuration and a prescribed initial stress state are derived. For convenience, tensor calculus has been used to derive the equations of motion. This was done in order to arrive at a compact formulation which could then be checked for consistency. The general tensor equations are then specialized for a shell of revolution with an arbitrary meridional configuration and are also cast into physical forms in order to obtain solutions to specific problems.

An approximate formulation of the equations of motion is discussed and a solution procedure for the asymmetric modes of free vibration is derived. The solution procedure is illustrated by means of several sample problems. The forced

---

[2]Numbers in parentheses refer to entries in the list of references in Appendix II.

response of these same shell problems is also studied.

EQUATIONS OF MOTION

The following assumptions were made in the derivation of the equations of motion for the superpositions of small oscillations about the initially-stressed configuration of a general shell:

1) The reference surface for the added deformations is taken as the initially-stressed middle surface.

2) The shell has negligible bending stiffness.

3) The thickness ratio = λ = *h/L is small compared to unity, where *h = one-half the shell thickness, and L = smallest characteristic length of the middle surface.

4) The shell material is perfectly elastic, homogenious and isotropic.

5) The additional oscillations are infinitesimal.

A special notation has been used to denote quantities defined on the additionally deformed shell. Given a function $f(x^\alpha)$ defined on the initially-stressed middle surface, the corresponding function on the additionally deformed middle surface is denoted by $[f(x^\alpha) + \epsilon' f'(x,^\alpha t)]$, where $\epsilon' f'(x^\alpha, t)$ = amount by which $[f(x^\alpha) + \epsilon' f'(x^\alpha, t)]$ differs from $f(x^\alpha, t)$, $x^\alpha (\alpha = 1,2)$ = middle surface coordinates, and where ϵ' = small non-dimensional parameter defined by the superposed additional load vector.

The equations of equilibrium for the additionally deformed surface, hereafter denoted by M', are formed by replacing the stresses acting on a shell element by their resultants acting on the corresponding element of M'. When this is done, the forces acting on M' are summed and are found to have the form

$$f_\circ(x^\alpha)(\epsilon')^\circ + f_1(x^\alpha, t)(\epsilon')^1 + f_2(x^\alpha, t)(\epsilon')^2 + \text{----} = 0$$

where the $f_\circ(x^\alpha)$ terms correspond to the equations of equilibrium for the initially-stressed middle surface and are therefore identically zero. According to assumption 5 above, all terms multiplied by $(\epsilon')^2$ and higher are neglected

compared to $f_2(x^\gamma,t)(\epsilon')^1$. The equations of motion are found to be (for a more detailed derivation see References 19 and 20):

$$\left[n'^{\alpha\gamma}\big|_\alpha + F'^\gamma - \frac{2\lambda\rho L^3}{*P}\frac{\partial^2 V'^\gamma_\circ}{\partial t^2}\right] + \left[n^{\rho\gamma}\Gamma'^\alpha_{\rho\alpha} + n^{\alpha\rho}\Gamma'^\gamma_{\rho\alpha}\right] = 0 \tag{1a}$$

$$\left[n'^{\alpha\gamma}B_{\alpha\gamma} + F'^3 - \frac{2\lambda\rho L^3}{*P}\frac{\partial^2 W'}{\partial t^2}\right] + \left[n^{\alpha\gamma}B'_{\alpha\gamma}\right] = 0 \tag{1b}$$

where covariant differentiation is denoted by a vertical line used as a subscript, and

$n^{\alpha\gamma} + \epsilon' n'^{\alpha\gamma}$ = force resultant tensor on M'

ρ = mass density of shell

$*P$ = largest characteristic force on the initially-stressed middle surface.

$L(\bar{F}+\epsilon'\bar{F}(t))$ = load vector on M' per unit area of M'

$= *P(F^\alpha+\epsilon' F'^\alpha)(\bar{A}_\alpha+\epsilon'A'_\alpha) + (F^3+\epsilon'F'^3)(\hat{N}+\epsilon'\bar{N}')$

$\bar{A}_\alpha + \epsilon'\bar{A}'_\alpha$ = base vectors of M'

$\hat{N} + \epsilon'\bar{N}'$ = unit normal vector to M'

$$\Gamma'^\rho_{\alpha\gamma} = 1/2\ A^{\beta\rho}\left[\frac{\partial A'_{\beta\alpha}}{\partial x^\alpha} + \frac{\partial A'_{\beta\gamma}}{\partial x^\alpha} - \frac{\partial A'_{\alpha\gamma}}{\partial x^\beta}\right] - A^{\beta\rho}\ A'_{\beta\sigma}\,{}^*\Gamma^\sigma_{\alpha\gamma}$$

$A_{\alpha\beta} + \epsilon' A'_{\alpha\beta}$ = metric tensor of M'

${}^*\Gamma^\sigma_{\alpha\gamma}$ = Christoffel symbols of the initially-stressed shell

$B_{\alpha\gamma} + \epsilon' B'_{\alpha\gamma}$ = curvature tensor of M'

$\epsilon' L\bar{V}'_\circ(t)$ = superposed displacement vector

$= \epsilon'(LV'^\gamma_\circ \bar{A}_\gamma + W'N)$

The effects of the initial stress state can be observed in Eqs. 1. They consist of the stress resultants $n^{\alpha\gamma}$ of the initially-stressed middle surface multiplied by functions of the added displacement vector. These terms have been grouped together within the second pairs of brackets in each equation.

Equation 1 can be expressed entirely in terms of displacement functions by substituting into Eqs. 1 the relations between the force resultants and the displacements.

$$*Pn'^{\alpha\gamma} = \frac{E\lambda L}{1+\nu}\left[A^{\alpha\rho}U'^{\gamma}_{\rho} + A^{\gamma\rho}U'^{\alpha}_{\rho} + \frac{2\nu}{1-\nu}A^{\alpha\gamma}U'^{\rho}_{\rho}\right] - *Pn^{\alpha\gamma}U'^{\rho}_{\rho} \tag{2}$$

where

E = Young's modulus $\qquad\qquad$ ν = Poisson's ratio

$$U'^{\gamma}_{\rho} = V'^{\gamma}_{\circ\alpha} - \frac{W'}{L}B^{\gamma}_{\alpha} \tag{3a}$$

$$U'^{3}_{\alpha} = \frac{\partial}{\partial x^{\alpha}}\left(\frac{W'}{L}\right) + V_{\circ}'^{\gamma}B_{\gamma\alpha} \tag{3b}$$

To complete the substitutions, the expressions for the additions to the metric tensor and the curvature tensor in terms of the added displacements are needed:

$$A'_{\alpha\gamma} = A_{\alpha\rho}U'^{\rho}_{\gamma} + A_{\gamma\rho}U'^{\rho}_{\alpha} \tag{4a}$$

$$B'_{\alpha\gamma} = 1/2\left[U'^{3}_{\alpha|\gamma} + U'^{3}_{\alpha|\gamma} + B_{\alpha\rho}U'^{\rho}_{\gamma} + B_{\gamma\rho}U'^{\rho}_{\alpha}\right. \tag{4b}$$

Once tensor forms of the equations of motion (Eqs. 1) have been expressed completely in terms of the additions to the displacement vector, it is necessary to cast them into physical forms in order to solve particular problems of interest. This is done via substitutions of the physical components for the various vectors on M'.

$$\frac{V'_{\circ}(\gamma)}{L} = V'^{\gamma}_{\circ}\sqrt{A_{\gamma\gamma}} \text{ (no sum)} \qquad \frac{V'_{\circ}(3)}{L} = \frac{W'}{L} \tag{5a}$$

$$N'_{(\alpha\gamma)} = *Pn'^{\alpha\gamma}\sqrt{A_{\gamma\gamma}A_{\alpha\alpha}} + 1/2N_{(\alpha\gamma)}\left[\frac{A'_{\gamma\gamma}}{A_{\gamma\gamma}} - \frac{A_{\alpha\alpha}}{A'_{\alpha\alpha}}\right] \text{ (no sum)} \tag{5b}$$

$$LP'_{(3)} = *PF'^{3} \qquad LP'_{(\alpha)} = *PF'^{\alpha}\sqrt{A_{\alpha\alpha}} + 1/2\,LP_{(\alpha)}\frac{A'_{\alpha\alpha}}{A_{\alpha\alpha}} \text{ (no sum)} \tag{5c}$$

where subscripts enclosed in parentheses denote physical components, and where $N_{(\alpha\gamma)}$, and $P_{(\alpha)}$ are the physical components of the initial stress resultants $n^{\alpha\gamma}$ and of the loads F^{α} required to obtain $N_{(\alpha\gamma)}$.

Shells of Revolution - The general equations of motion can be specialized for a shell of revolution with an arbitrary meridional contour (Fig. 1). The middle surface coordinates are defined as follows: x^1 = regular meridional

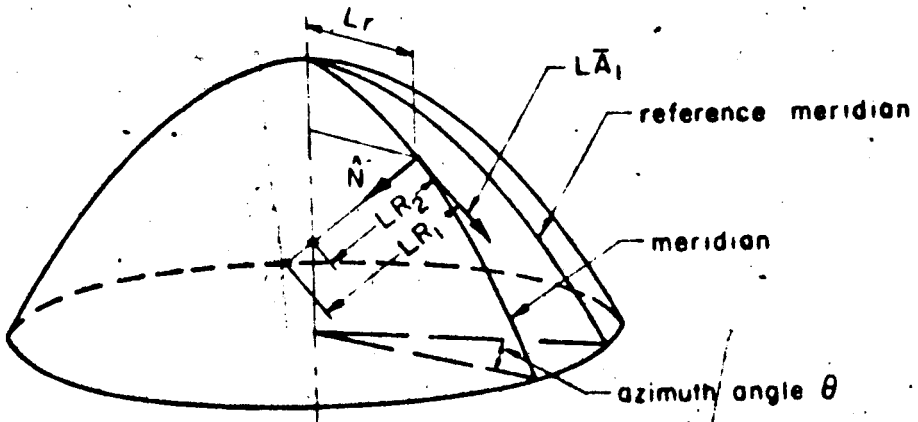

Fig #1

Leonard

coordinate, e.g. arc length; and x^2 = azimuth angle θ.

Asymmetric oscillations about an axially-symmetric initial stress state have been considered. Therefore, derivatives with respect to θ of all quantities associated with the initially-stressed shell of revolution are identically zero. For quantities associated with the additional deformations, $\partial f(x^1,\theta)/\partial x^1$ is denoted by $f(x^1,\theta)$, and $\partial f(x^1,\theta)/\partial\theta$ by $f(x^1,\theta)$. Also, it is convenient to make a change of notation: let

$$u = V'_{o(1)}/L \qquad v = V'_{o(2)}/L \qquad w = V'_{o(3)}/L \tag{6}$$

The physical forms of Eqs. 1 specialized for a general shell of revolution are

$$\begin{aligned}
&\hat{\tilde{u}}\left[1 + K_1\right] + \hat{\tilde{v}}\left[\frac{1+\nu}{2}\right]\frac{\sqrt{A_{11}}}{r} + \tilde{\hat{u}}\left[\frac{1-\nu}{2} + K_2\right]\frac{A_{11}}{r^2} + \hat{u}\left[\frac{\hat{\lambda}}{\lambda} - \frac{\hat{A}_{11}}{2A_{11}} + \frac{\hat{r}}{r}\right.\\
&\left. - K_1\frac{\hat{A}_{11}}{2A_{11}} + K_2\frac{\hat{r}}{r}\right] + \tilde{\hat{v}}\left[\frac{\hat{\lambda}}{\lambda}\nu - \frac{3-\nu}{2}\frac{\hat{r}}{r} - K_2\frac{2\hat{r}}{r}\right.\\
&\left. + \frac{LP_{(1)}}{K}\sqrt{A_{11}}\right]\frac{\sqrt{A_{11}}}{r} - \hat{w}\left[\frac{R_2 + \nu R_1}{R_1R_2} + \frac{K_1}{R_1} - \frac{K_2}{R_2}\right]\sqrt{A_{11}} + u\left[\frac{\hat{\lambda}}{\lambda}\frac{\hat{r}}{r}\nu\right.\\
&\left. + \nu\frac{\hat{\hat{r}}}{r} - \frac{\hat{r}^2}{r^2} - \nu\frac{\hat{A}_{11}}{2A_{11}}\frac{\hat{r}}{r} - K_2\left(\frac{\hat{\hat{r}}}{r} + \frac{\hat{r}^2}{r^2} - \frac{\hat{A}_{11}}{2A_{11}}\frac{\hat{r}}{r}\right) + \frac{LP_{(1)}}{K}\sqrt{A_{11}}\frac{\hat{r}}{r}\right]\\
&+ w\left[\frac{\hat{R}_1}{R_1^2} + \nu\frac{\hat{R}_2}{R_2^2} - \frac{\hat{\lambda}}{\lambda}\frac{R_2+\nu R_1}{R_1R_2} + \frac{1-\nu}{r}\hat{r}\frac{R_1-R_2}{R_1R_2} + K_1\frac{\hat{R}_1}{R_1^2} + K_2\left(\frac{2\hat{r}}{r}\frac{R_1-R_2}{R_1R_2}\right.\right.\\
&\left.\left. - \frac{\hat{R}_2}{R_2^2}\right) - \frac{LP_{(1)}\sqrt{A_{11}}}{KR_2}\right]\sqrt{A_{11}} + \frac{LP'_{(1)}}{K}A_{11} - \frac{2\lambda_o L^3}{K}A_{11}\frac{\partial^2 u}{\partial t^2} = 0
\end{aligned} \tag{7a}$$

$$\begin{aligned}
&\tilde{\hat{u}}\left[\frac{1+\nu}{2}\right] + \hat{\hat{v}}\left[\frac{1-\nu}{2} + K_1\right]\frac{r}{\sqrt{A_{11}}} + \tilde{\hat{v}}\left[1 + K_2\right]\frac{\sqrt{A_{11}}}{r} + \tilde{u}\left[\frac{1-\nu}{2}\frac{\hat{\lambda}}{\lambda} + \frac{\hat{r}}{r}\right.\\
&\left. + K_2\,2\frac{\hat{r}}{r}\right] + \hat{v}\left[\frac{1-\nu}{2}\left(\frac{\hat{\lambda}}{\lambda} - \frac{\hat{A}_{11}}{2A_{11}} + \frac{\hat{r}}{r}\right) - K_1\frac{\hat{A}_{11}}{2A_{11}} + K_2\frac{\hat{r}}{r}\right]\frac{r}{\sqrt{A_{11}}}\\
&+ v\left[\frac{1-\nu}{2}\left(\frac{\hat{\hat{r}}}{r} + \frac{\hat{r}^2}{r^2} + \frac{\hat{r}}{r}\frac{\hat{\lambda}}{\lambda} - \frac{\hat{r}}{r}\frac{\hat{A}_{11}}{2A_{11}}\right) + K_1\left(\frac{\hat{\hat{r}}}{r} - \frac{\hat{A}_{11}}{2A_{11}}\frac{\hat{r}}{r}\right) + K_2\frac{\hat{r}^2}{r^2}\right]\frac{r}{\sqrt{A_{11}}}\\
&- \tilde{w}\left[\frac{R_1+\nu R_2}{R_1R_2} - \frac{K_1}{R_1} + \frac{K_2}{R_2}\right]\sqrt{A_{11}} + \frac{LP'_{(2)}}{K}r\sqrt{A_{11}} - \frac{2\lambda_o L^3}{K}r\sqrt{A_{11}}\frac{\partial^2 v}{\partial t^2} = 0
\end{aligned} \tag{7b}$$

$$\hat{\hat{w}}\left[\frac{K_1}{\sqrt{A_{11}}}\right] + \tilde{\tilde{w}}\left[\frac{K_2}{r}\right]\frac{\sqrt{A_{11}}}{r} + \hat{u}\left[\frac{R_2+\nu R_1}{R_1R_2} + \frac{K_1}{R_1} - \frac{K_2}{R_2}\right] + \tilde{v}\left[\frac{R_1+\nu R_2}{R_1R_2}\right.$$

$$\left. - \frac{K_1}{R_1} + \frac{K_2}{R_2}\right]\frac{\sqrt{A_{11}}}{r} - \hat{w}\left[K_1\frac{\hat{A}_{11}}{2A_{11}} - K_2\frac{\hat{r}}{r}\right]\frac{1}{\sqrt{A_{11}}} + u\left[\frac{\hat{r}}{r}\frac{R_1+\nu R_2}{R_1R_2}\right.$$

$$\left. - \frac{K_1}{R_1}\left(\frac{\hat{R}_1}{R_1} + \frac{\hat{r}}{r}\right) + \frac{K_2}{R_2}\frac{\hat{r}}{r}\right] - w\left[\frac{R_2+\nu R_1}{R_1} + \frac{R_1+\nu R_2}{R_2} - K_1 - K_2\right]\frac{\sqrt{A_{11}}}{R_1R_2}$$

$$+ \frac{LP'(3)}{K}\sqrt{A_{11}} - \frac{2\lambda_0 L^3}{K}\sqrt{A_{11}}\frac{\partial^2 w}{\partial t^2} = 0 \qquad (7c)$$

where:

$$K = \frac{2E\lambda L}{1-\nu^2} \qquad K_2 = \frac{N_{(11)}}{K} \qquad K_2 = \frac{N_{(22)}}{K}$$

r = perpendicular distance of a point on the initially-stressed middle surface from the axis of revolution

R_1, R_2 = non-dimensional radii of curvature of the initially-stressed shell

If Eqs. (7) are rearranged it is possible to segregate the effects of the initial stress state as follows:

$$0 = \{\text{...classical membrane equations of motion...}\}$$

$$+ N_{(11)}\{\text{...functions of the added displacements...}\}$$

$$+ N_{(22)}\{\text{...functions of the added displacements...}\}$$

An approximate formulation of Eqs. 7 is discussed in Reference 20. In that approximate theory for initially-stressed shells, it was shown that the effects of the initial stress can be neglected in the first two of the equations of motion, Eqs. 7a and 7b. However, in the third equation of motion, Eq. 7c, the initial stress components should be retained in order to adequately describe the shell behavior in the neighborhood of discontinuities and non-membrane type boundaries. The approximate formulation of the equations of motion for a general shell of revolution is

$$\hat{\hat{u}} + \tilde{\tilde{v}}\frac{1+2}{2}\frac{\sqrt{A_{11}}}{r} + \tilde{u}\frac{1-\nu}{2}\frac{A_{11}}{r^2} + \hat{u}\left[\frac{\hat{\Delta}}{\lambda} - \frac{\hat{A}_{11}}{2A_{11}} + \frac{\hat{r}}{r}\right] + \tilde{v}\left[\nu\left(\frac{\hat{\Delta}}{\lambda} - \frac{3-\nu}{2}\frac{\hat{r}}{r}\right]\frac{\sqrt{A_{11}}}{r}\right.$$

$$- \hat{w}\frac{R_2+\nu R_1}{R_1R_2}\sqrt{A_{11}} + u\left[\nu\left(\frac{\hat{\lambda}}{\lambda}\frac{\hat{r}}{r} + \frac{\hat{\hat{r}}}{r} - \frac{\hat{A}_{11}}{2A_{11}}\frac{\hat{r}}{r}\right) - \frac{\hat{r}^2}{r^2}\right] + w\left[\frac{\hat{R}_1}{R_1^2} + \nu\frac{\hat{R}_2}{R_2^2} - \frac{\hat{\lambda}}{\lambda}\frac{R_2+\nu R_1}{R_1R_2}\right.$$

$$\left. + \frac{1-\nu}{r}\hat{r}\frac{R_1-R_2}{R_1R_2}\right]\sqrt{A_{11}} + \frac{LP'(1)}{K}A_{11} - \frac{2\lambda\rho L^3}{K}A_{11}\frac{\partial^2 u}{\partial t^2} = 0 \qquad (8a)$$

$$\tilde{\hat{u}}\frac{1+\nu}{2} + \hat{\hat{v}}\frac{1-\nu}{2}\frac{r}{\sqrt{A_{11}}} + \tilde{\approx v}\frac{\sqrt{A_{11}}}{r} + \tilde{u}\left[\frac{1-\nu}{2}\frac{\hat{\lambda}}{\lambda} + \frac{\hat{r}}{r}\right] + \hat{v}\frac{1-\nu}{2}\left[\frac{\hat{\lambda}}{\lambda} + \frac{\hat{r}}{r}\right.$$

$$\left. - \frac{\hat{A}_{11}}{2A_{11}}\right]\frac{r}{\sqrt{A_{11}}} - v\frac{1-\nu}{2}\left[\frac{\hat{\hat{r}}}{r} + \frac{\hat{r}^2}{r^2} + \frac{\hat{r}}{r}\frac{\hat{\lambda}}{\lambda} - \frac{\hat{r}}{r}\frac{\hat{A}_{11}}{2A_{11}}\right]\frac{r}{\sqrt{A_{11}}} - \tilde{w}\frac{R_1+\nu R_2}{R_1R_2}\sqrt{A_{11}}$$

$$+ \frac{LP'(2)}{K}r\sqrt{A_{11}} - \frac{2\lambda\rho L^3}{K}r\sqrt{A_{11}}\frac{\partial^2 v}{\partial t^2} = 0 \qquad (8b)$$

$$\hat{\approx w}\frac{K_1}{\sqrt{A_{11}}} + \tilde{\approx w}\frac{K_2}{r}\frac{\sqrt{A_{11}}}{r} + \hat{u}\left[\frac{R_2+\nu R_1}{R_1R_2} + \frac{K_1}{R_1} - \frac{K_2}{R_2}\right] + \tilde{v}\left[\frac{R_1+\nu R_2}{R_1R_2} - \frac{K_1}{R_1}\right.$$

$$\left. + \frac{K_2}{R_2}\right]\frac{\sqrt{A_{11}}}{r} - \frac{\hat{w}}{\sqrt{A_{11}}}\left[K_1\frac{\hat{A}_{11}}{2A_{11}} - K_2\frac{\hat{r}}{r}\right] + u\left[\frac{\hat{r}}{r}\frac{R_1+\nu R_2}{R_1R_2} - \frac{K_1}{R_1}\left(\frac{\hat{R}_1}{R_1}\right.\right.$$

$$\left.\left. + \frac{\hat{r}}{r}\right) + \frac{K_2}{R_2}\frac{\hat{r}}{r}\right] - w\left[\frac{R_2+\nu R_1}{R_1} + \frac{R_1+\nu R_2}{R_2} - K_1 - K_2\right]\frac{\sqrt{A_{11}}}{R_1R_2}$$

$$+ \frac{LP'(3)}{K}\sqrt{A_{11}} - \frac{2\lambda\rho L^3}{K}\sqrt{A_{11}}\frac{\partial^2 w}{\partial t^2} = 0 \qquad (8c)$$

It was shown in Reference 20 that the approximate static equations equivalent to Eqs. 8 gave solutions in close agreement with the solutions to the more exact formulation. Also, both of those solutions were significantly different from the solutions to the equivalent classical membrane equations where the effects of initial stress are ignored. In a succeeding section, the solutions to both the approximate and the exact equations, Eqs. 8 and 7 respectively, will be compared for several sample dynamic problems.

SOLUTION TECHNIQUE: FREE VIBRATION

In the consideration of the natural frequencies and associated mode shapes for the asymmetric superposed equations of motion, all the forcing functions

$P'_{(1)}$, $P'_{(2)}$, and $P'_{(3)}$ are assumed to be zero and the displacements to be harmonic functions

$$u(x^1, \theta, t) = u^*(x^1, \theta)\, e^{i\omega t} \tag{9a}$$

$$v(x^1, \theta, t) = v^*(x^1, \theta)\, e^{i\omega t} \tag{9b}$$

$$w(x^1, \theta, t) = w^*(x^1, \theta)\, e^{i\omega t} \tag{9c}$$

If in addition, the functions u*, v*, w*, are expanded in Fourier Series, it can be seen that Eqs. 7 and 8 admit solutions of the form (torsional vibrations are ignored):

$$u^*(x^1, \theta) = \sum_{n=0}^{\infty} u^n(x^1) \cos n\theta \tag{10a}$$

$$v^*(x^1, \theta) = \sum_{n=0}^{\infty} v^n(x^1) \sin n\theta \tag{10b}$$

$$w^*(x^1, \theta) = \sum_{n=0}^{\infty} w^n(x^1) \cos n\theta \tag{10c}$$

If Eqs. 9 and 10 are substituted into Eqs. 7, an infinite set of ordinary differential equations results, each set of which has the form

$$\begin{aligned} 0 = {} & \hat{u}^n \left[1 + K_1\right] + \hat{u}^n \left[\frac{\hat{\lambda}}{\lambda} + \frac{\hat{r}}{r} - \frac{\hat{A}_{11}}{2A_{11}} - K_1 \frac{\hat{A}_{11}}{2A_{11}} + K_2 \frac{\hat{r}}{r}\right] - \hat{w}^n\left[\frac{R_2+\nu R_1}{R_1 R_2} + \frac{K_1}{R_1}\right. \\ & \left. - \frac{K_2}{R_2}\right] \sqrt{A_{11}} + n\hat{v}^n \frac{1+\nu}{2} \frac{\sqrt{A_{11}}}{r} + u^n\left[\nu \frac{\hat{\lambda}}{\lambda} \frac{\hat{r}}{r} + \nu \frac{\hat{\hat{r}}}{r} - \nu \frac{\hat{A}_{11}}{2A_{11}} \frac{\hat{r}}{r} - \frac{\hat{r}^2}{r^2} - n^2 \frac{1-\nu}{2} \frac{A_{11}}{r^2}\right. \\ & \left. + K_2 \left(\frac{\hat{A}_{11}}{2A_{11}} \frac{\hat{r}}{r} - \frac{\hat{\hat{r}}}{r} + \frac{\hat{r}^2}{r^2} - n^2 \frac{A_{11}}{r^2}\right) + G \frac{\hat{r}}{r} + pA_{11}\right] + nv^n\left[\nu \frac{\hat{\lambda}}{\lambda} - \frac{3-\nu}{2} \frac{\hat{r}}{r}\right. \\ & \left. - 2K_2 \frac{\hat{r}}{r} + G\right] \frac{\sqrt{A_{11}}}{r} + w^n\left[\frac{\hat{R}_1}{R_1^2} + \nu \frac{\hat{R}_2}{R_1^2} - \frac{\hat{\lambda}}{\lambda} \frac{R_2+\nu R_1}{R_1 R_2} + \frac{1-\nu}{r} \hat{r} \frac{R_1-R_2}{R_1 R_2} + K_1 \frac{\hat{R}_1}{R_1^2}\right. \\ & \left. + K_2 \left(2\frac{\hat{r}}{r} \frac{R_1-R_2}{R_1 R_2} - \frac{\hat{R}_2}{R_2^2}\right) - \frac{G}{R_2}\right] \sqrt{A_{11}} \end{aligned} \tag{11a}$$

$$0 = \hat{v}^n\left[\frac{1-\nu}{2} + K_1\right] \frac{r}{\sqrt{A_{11}}} + \hat{v}^n\left[\frac{1-\nu}{2}\left(\frac{\hat{\lambda}}{\lambda} - \frac{\hat{A}_{11}}{2A_{11}} + \frac{\hat{r}}{r}\right) - K_1 \frac{\hat{A}_{11}}{2A_{11}} + K_2 \frac{\hat{r}}{r}\right] \frac{r}{\sqrt{A_{11}}}$$

$$- n\hat{u}^n \frac{1+\nu}{2} - nu^n\left[\frac{1-\nu}{2}\frac{\hat{\lambda}}{\lambda} + \frac{3-\nu}{2}\frac{\hat{r}}{r} + 2K_2\frac{\hat{r}}{r}\right] - v^n\left[\frac{1-\nu}{2}\left(\frac{\hat{\hat{r}}}{r} + \frac{\hat{r}^2}{r^2} + \frac{\hat{\lambda}}{\lambda}\frac{\hat{r}}{r} - \frac{\hat{r}}{r}\frac{\hat{A}_{11}}{2A_{11}}\right)\right.$$

$$\left. + n^2\frac{A_{11}}{r^2} + K_1\left(\frac{\hat{\hat{r}}}{r} - \frac{\hat{A}_{11}}{2A_{11}}\frac{\hat{r}}{r}\right) + K_2\left(\frac{\hat{r}^2}{r^2} + n^2\frac{A_{11}}{r^2}\right) - pA_{11}\right]\frac{r}{\sqrt{A_{11}}}$$

$$+ nw^n\left[\frac{R_1+\nu R_2}{R_1R_2} - \frac{K_1}{R_1} + \frac{K_2}{R_2}\right]\sqrt{A_{11}} \qquad (11b)$$

$$0 = \hat{w}^n\frac{K_2}{\sqrt{A_{11}}} + \hat{u}^n\left[\frac{R_2+\nu R_1}{R_1R_2} + \frac{K_1}{R_1} - \frac{K_2}{R_2}\right] + \frac{\hat{w}^n}{\sqrt{A_{11}}}\left[K_2\frac{\hat{r}}{r} - K_1\frac{\hat{A}_{11}}{2A_{11}}\right] + u^n\left[\frac{\hat{r}}{r}\frac{R_1+\nu R_2}{R_1R_2}\right.$$

$$\left. - \frac{K_1}{R_1}\left(\frac{\hat{R}_1}{R_1} + \frac{\hat{r}}{r}\right) + \frac{K_2}{R_1}\frac{\hat{r}}{r}\right] + nv^n\left[\frac{R_1+\nu R_2}{R_1R_2} - \frac{K_1}{R_1} + \frac{K_2}{R_2}\right]\frac{\sqrt{A_{11}}}{r} - w^n\left[\frac{R_2+\nu R_1}{R_1} + \frac{R_1+\nu R_2}{R_2}\right.$$

$$\left. - K_1 - K_2\left(1 - \frac{R_1R_2}{r^2}n^2\right) - R_1R_2p\right]\frac{\sqrt{A_{11}}}{R_1R_2} \qquad (11c)$$

where

$$G = \frac{LP_{(1)}\sqrt{A_{11}}}{K} \qquad p = \frac{\rho L^2(1-\nu^2)}{E}\omega^2 \qquad (11d)$$

If the approximate equations of motion, Eqs. 8, are considered, the set of ordinary differential equations equivalent to the exact theory, Eqs. 11, are as follows:

$$0 = \hat{u}^n + \hat{u}^n\left[\frac{\hat{\lambda}}{\lambda} + \frac{\hat{r}}{r} - \frac{\hat{A}_{11}}{2A_{11}}\right] - \hat{w}^n\frac{R_2+\nu R_1}{R_1R_2}\sqrt{A_{11}} + n\hat{v}^n\frac{1+\nu}{2}\frac{\sqrt{A_{11}}}{r} + u^n\left[\nu\left(\frac{\hat{\lambda}}{\lambda}\frac{\hat{r}}{r} + \frac{\hat{\hat{r}}}{r}\right.\right.$$

$$\left.\left. - \frac{\hat{A}_{11}}{2A_{11}}\frac{\hat{r}}{r}\right) - \frac{\hat{r}^2}{r^2} - n^2\frac{1-\nu}{2}\frac{A_{11}}{r^2} + G\frac{\hat{r}}{r} + pA_{11}\right] + nv^n\left[\nu\frac{\hat{\lambda}}{\lambda} - \frac{3-\nu}{2}\frac{\hat{r}}{r} + G\right]\frac{\sqrt{A_{11}}}{r}$$

$$+ w^n\left[\frac{\hat{R}_1}{R_1} + \nu\frac{\hat{R}_2}{R_2} - \frac{\hat{\lambda}}{\lambda}\frac{R_2+\nu R_1}{R_1R_2} + \frac{1-\nu}{r}\hat{r}\frac{R_1-R_2}{R_1R_2} - \frac{G}{R^2}\right]\sqrt{A_{11}} \qquad (12a)$$

$$0 = \hat{v}^n\frac{1-\nu}{2}\frac{r}{\sqrt{A_{11}}} + \hat{v}^n\frac{1-\nu}{2}\left[\frac{\hat{\lambda}}{\lambda} - \frac{\hat{A}_{11}}{2A_{11}} + \frac{\hat{r}}{r}\right]\frac{r}{\sqrt{A_{11}}} - n\hat{u}\frac{1+\nu}{2} - nu^n\left[\frac{1-\nu}{2}\frac{\hat{\lambda}}{\lambda} + \frac{3-\nu}{2}\frac{\hat{r}}{r}\right]$$

$$+ nw^n\frac{R_1+\nu R_2}{R_1R_2}\sqrt{A_{11}} - v^n\left[\frac{1-\nu}{2}\left(\frac{\hat{\hat{r}}}{r} + \frac{\hat{r}^2}{r^2} + \frac{\hat{\lambda}}{\lambda}\frac{\hat{r}}{r} - \frac{\hat{r}}{r}\frac{\hat{A}_{11}}{2A_{11}}\right) + n^2\frac{A_{11}}{r^2} + pA_{11}\right]\frac{r}{\sqrt{A_{11}}} \qquad (12b)$$

$$0 = \hat{w}^n\frac{K_2}{\sqrt{A_{11}}} + \hat{u}^n\left[\frac{R_2+\nu R_1}{R_1R_2} + \frac{K_1}{R_1} - \frac{K_2}{R_2}\right] + \frac{w^n}{\sqrt{A_{11}}}\left[K_2\frac{\hat{r}}{r} - K_1\frac{\hat{A}_{11}}{2A_{11}}\right] + u^n\left[\frac{r}{r}\frac{R_1+\nu R_2}{R_1R_2}\right.$$

$$\frac{K_1}{R_1}\left(\frac{\hat{R}_1}{R_1}+\frac{\hat{r}}{r}\right)+\frac{K_2}{R_1}\frac{\hat{r}}{r}\Big] + nv^n\Big[\frac{R_1+\nu R_2}{R_1R_2}-\frac{K_1}{R_1}+\frac{K_2}{R_2}\Big]\frac{\sqrt{A_{11}}}{r} - w^n\Big[\frac{R_2+\nu R_1}{R_1}+\frac{R_1+\nu R_2}{R_2}$$

$$- K_1 - K_2\left(1-\frac{R_1R_2}{r^2}n^2\right) - R_1R_2P\Big]\frac{\sqrt{A_{11}}}{R_1R_2} \qquad (12c)$$

Determination of Eigenvalues - The method used to determine the natural frequencies and mode shapes for the asymmetric vibrations of initially-stressed shells is (1) to select a trial value for the natural frequency ω, and to check if the trial value provides an unique solution which satisfies the equations of motion (Eqs. 11 or 12) and their associated homogenious boundary conditions. If the trial value of ω were a natural frequency, a non-trivial family of solutions which differ only by a multiplicative constant would have been found.

When the trial ω is substituted into the equations of motion, the combined initial-value and boundary-value problem is converted into an equivalent boundary-value problem for which one method of solution has been discussed previously (20). This solution method is reviewed below. The trial frequencies are tested by calculating a determinant associated with the equivalent static solution. Since the elements of this determinant (described below) are continuous functions of ω, a change in sign of the determinant for two different trial values of ω implies the existence of a natural frequency between those two trial values. Then using binary search techniques, one can obtain better approximations to the natural frequency.

Boundary Conditions - The solutions to the combined initial-value and boundary-value problem posed by either of Eqs. 11 or 12 can be obtained if the initial conditions and six boundary conditions for each value of n are correctly prescribed. The three boundary conditions at an edge of the shell can in most cases be readily obtained using Fourier expansions.

The criteria for establishment of boundary conditions in the particular case of a shell continuous at the apex are such that there exists no singularity

at the apex (20, 31). Since the solutions u^n, v^n, w^n are analytic functions at the apex, it is possible to obtain solutions to either Eqs. 11 or 12 in the neighborhood of $x^1 = 0$ (regular single point) by means of series expansions. When the series expansions of u^n, v^n, w^n are substituted into the equations of motion evaluated at $x^1 = 0$, certain relations between the constants of the series expansions are obtained which must be satisfied in order to satisfy equilibrium at the apex. These relations can be considered as apex boundary conditions for the numerical integration of the boundary-value problem equivalent to Eqs. 11 or 12.

Let x^1 be φ, the angle that the normal to the shell makes with the axis of revolution. The Taylor series expansions of u^n, v^n and w^n about the point $\varphi = 0$ are

$$u^n = \sum_{m=0}^{\infty} a_m^n \varphi^m \tag{13a}$$

$$v^n = \sum_{m=0}^{\infty} b_m^n \varphi^m \tag{13b}$$

$$w^n = \sum_{m=0}^{\infty} c_m^n \varphi^m \tag{13c}$$

If Eqs. 13 are substituted into either of Eqs. 11 or 12 and if terms are collected in powers of φ, the vanishing of all terms independently of φ yields the following set of relations between the constants of the series expansions (different relations are obtained for each value of n; only the relationships for n = 0, 1, 2 are listed here)

<u>n = 0</u> (a_1°, b_1°, $c_\circ^\circ$ arbitrary)

$$a_\circ^\circ = b_\circ^\circ = c_1^\circ = a_2^\circ = b_2^\circ = c_3^\circ = 0 \tag{14a}$$

$$c_2^\circ = \frac{2(1+\nu)\,(c_\circ^\circ - a_1^\circ) - (pR_1^2 + 2K_1)\,c_\circ^\circ}{4K_1} \tag{14b}$$

$$a_3^\circ = \frac{2(1+\nu)\,c_2^\circ - \left(\frac{1-3\nu}{3} + \frac{4K_1}{3} + pR_1^2\right) a_1^\circ}{8(1+K_1)} \tag{14c}$$

$$b_3^\circ = -\left[1 + \frac{6pR_1^2}{4-4\nu+8K_1}\right] \frac{b_1^\circ}{6} \tag{14d}$$

a_m°, b_m°, c_m° determined by a_1°, b_1°, $c_\circ^\circ$ for $m \geq 2$

$\underline{n = 1}$ $(a_2^1,\ b_0^1,\ c_1^1$ arbitrary)

$$c_0^1 = a_1^1 = b_1^1 = c_2^1 = a_3^1 = b_3^1 = 0 \tag{15a}$$

$$a_0^1 = -\,b_0^1 \tag{15b}$$

$$b_2^1 = \frac{\left(\frac{5+\nu}{2} + 2K_1\right) a_2^1 - (1+\nu)\, c_1^1 - \left(\frac{1-3\nu}{4} + pR_1^2 + K_1\right) b_0^1}{\frac{1-3\nu}{2} + 2K_1} \tag{15c}$$

$$c_3^1 = \frac{\left[2(1+\nu) - pR_1^2 - \frac{4K_1}{3}\right] c_1^1 - (1+\nu)\,(3c_2^1 + b_2^1) + \frac{1+\nu}{2}\, b_0^1}{8K_1} \tag{15d}$$

$a_m^1,\ b_m^1,\ c_m^1$ determined by $a_2^1,\ b_0^1,\ c_1^1$ for $m \geq 3$

$\underline{n = 2}$ $(a_3^2,\ b_1^2,\ c_2^2$ arbitrary)

$$a_0^2 = b_0^2 = c_0^2 = c_1^2 = a_2^2 = b_2^2 = c_3^2 = 0 \tag{16a}$$

$$a_1^2 = -b_1^2 \tag{16b}$$

$$b_3^2 = \frac{\frac{3+\nu+2K_1}{2}\left(a_3^2 + \frac{b_1^2}{6}\right) - \frac{1+\nu}{2}\, c_2^2}{K_1 - \nu} \tag{16c}$$

$a_m^2,\ b_m^2,\ c_m^2$ determined by $a_3^2,\ b_1^2,\ c_2^2$ for $m \geq 4$

Numerical Integration Scheme - The method of solution chosen for the boundary-value problem posed by either Eqs. 11 or 12 is a generalization of Holzer's method (3, 8, 12, 25, 31) in which the two-point boundary-value problem is transformed into a set of homogeneous initial-value problems, each initial-value problem being integrated numerically using a generalized trapezoidal rule. The proper initial conditions for each initial-value problem are formed by assuming independent values of the unknown derivatives at one boundary of the shell. Since Eqs. 11 and 12 are both sixth-order systems with three boundary conditions prescribed at each end of a typical meridional line, three independent assumptions can be made for the initial conditions for each of the three homogeneous

initial-value problems.

The solution process for the two-point boundary-value problem is outlined below:

1. For an assumed value of ω, the 6th-order boundary-value problem is transformed into 3 initial-value problems by assuming 3 independent sets of homogeneous boundary conditions at one edge of the shell.

2. The solution to each homogeneous initial-value problem is propagated along a typical meridian. Newmark's beta-method, a generalized trapezoidal rule for intigration, is used. See References 19, 20, 25 for discussions and applications of this method. Three partial solutions are thus generated.

3. The total solution at any meridional point, including the boundary, is a linear combination of the three partial solutions:

$$\left\{\begin{matrix}\text{true}\\ \text{solution}\end{matrix}\right\} = \left[\begin{matrix}\text{partial}\\ \text{solutions}\end{matrix}\right] \left\{\begin{matrix}\alpha_1\\ \alpha_2\\ \alpha_3\end{matrix}\right\} \tag{17}$$

where α_i are the constants of the combination.

4. In order that the homogeneous boundary conditions at the edge be satisfied, the linear homogeneous equations formed from the corresponding portions of the partial solutions must have a non-trivial solution. In other words, the determinate of the coefficient matrix for the partial solutions corresponding to the boundary conditions must be zero.

$$\left\{\begin{matrix}\text{true}\\ \text{boundary}\\ \text{conditions}\end{matrix}\right\} = \left[\begin{matrix}\text{boundary values}\\ \text{for}\\ \text{partial solutions}\end{matrix}\right] \left\{\begin{matrix}\alpha_1\\ \alpha_2\\ \alpha_3\end{matrix}\right\} = \left\{\begin{matrix}0\\ 0\\ 0\end{matrix}\right\} \tag{18}$$

$$\therefore \quad \det \left| \begin{matrix}\text{boundary values}\\ \text{for}\\ \text{partial solutions}\end{matrix} \right| = 0$$

5. If the determinant is not zero, the trial value of ω is not a natural frequency and steps 1 to 3 must be repeated for another trial value. After two values of ω are found for which the signs of the corresponding determinant are oppisite, a half-interval search is instituted to find the bracketed value of ω corresponding to a natural frequency.

6. If the determinant is zero, the boundary conditions are satisfied and the mode shape for that natural frequency is determinable to within an arbitrary constant by solving Eq. 18 for α_2 and α_3 in terms of α_1 and then by combining the partial solutions as in Eq. 17.

If the starting point for the numerical integration of the initial-value problems is the apex, special methods must be used in the neighborhood of the apex. The solutions in the region of $\varphi = 0$ are approximated by Taylor series expansions, Eqs. 13. For any value of n, sufficient terms in the series expansions must be taken such that all of the arbitrary constants in Eqs. 14, 15, and 16 are included. This will guarantee that the solutions at all points in the shell are linear combinations of all the arbitrary conditions at the apex (20, 31).

Since it is not possible to consider all terms in the Taylor series expansions, it is necessary to use a successive approximation scheme for propagating solutions in the neighborhood of the apex. Such a scheme is described in Reference 20. It was found that in cases where the geometry of the shell changes rapidly near the apex, e.g. a paraboloid, more rapid convergence of the successive approximations was possible if, instead of using Taylor expansions of the displacement functions (u, v, w), Taylor expansions of u/R_1, v/r, and w were used.

Suppression of Extraneous Solutions. - The use of the generalized Holzer method in cases where the numerical integration must proceed over a long interval introduces serious convergence difficulties in that the solution to each of the initial-value problems includes both a decaying function of x^1 and a rapidly growing function of x^1 (9). The coefficient of the rapidly growing function should in theory be zero, but because of various numerical integration errors is not exactly zero. For short regions of integration the rapidly growing extraneous solutions have negligible effect on the combination of the partial

solutions. However, for longer intervals of integration, the extraneous solutions predominate and the equations which express the linear combinations of the partial solutions are extremely ill-conditioned.

There are two methods in current use for alleviating this convergence problem. One method, the multi-segment method, consists of subdividing the shell region into short segments (4, 14, 15, 21). The initial-value problems are integrated within each segment, and solutions are combined to satisfy compatibility requirements at the junctions of the various segments. The second method, the suppression method, consists of combining the partial solutions at selected points along the meridian in order to suppress the extraneous solutions (3, 8, 30, 31). Although the two methods are similar in concept, and although the multi-segment method lends itself to an easier physical interpretation, the suppression method requires a lesser number of independent partial solutions. Also, instead of solving, for example, one set of 3N equations simultaneously, N sets of 3 simultaneous equations are solved successively. For the above reasons the suppression method was chosen in this study.

The suppression method is implemented by requiring that at certain meridional points fictitious conditions be satisfied by linear combinations of the unsuppressed partial solutions. The fictitious conditions to be satisfied must be arbitrary, independent conditions which have small magnitudes compared with the partial solutions. The partial solutions are therefore combined to form new arbitrary partial solutions in which the extraneous growing functions are suppressed. The linear combinations at the point of suppression and at all prior points constitute the new set of arbitrary solutions which are then propagated along the meridian to the next point at which suppression is required. The suppression process is detailed in References 3 and 30.

SAMPLE SOLUTIONS: FREE VIBRATIONS

In order to test the solution procedures described in the previous section for both the exact and the approximate equations of motion (Eqs. 11 and 12), several illustrative examples were solved for their natural frequencies and mode shapes, only the n = 0, 1, 2 harmonics being considered. A computer program was developed which was capable of handling a shell of revolution with a general meridional configuration. The program was tested on several sample shell configurations including: a sphere continuous at the apex and fixed or simply-supported at the base; a sphere fixed or simply-supported near the apex and at the base; a sphere with a rigid plug near the apex and fixed at the base; a paraboloid of revolution continuous at the apex and fixed or simply-supported at the base; a toroidal section with a rigid plug at one end and fixed at the other end. The results for several of these problems are presented in this section.

Sphere Continuous at Apex. - The first example considered was an initially-stressed spherical segment fixed at its base as shown in Fig. 2a. The initial stress state was attained via internal pressure $\bar{p}$, the smallest characteristic length L = radius of sphere, and φ_o = opening angle of the sphere. If the following substitutions are made in Eqs. 11 or 12, the natural frequencies and associated mode shapes for this problem can be obtained:

$$x^1 = \varphi \qquad G = 0 \qquad r = R \sin\varphi \tag{19a}$$

$$K_1 = K_2 = \frac{\bar{p} R (1-\nu^2)}{4E\lambda} \qquad R_1 = R_2 = \sqrt{A_{11}} = R \tag{19b}$$

Several numerical problems were considered. Figures 3, 4, and 5 depict the first three natural displacement and stress mode shapes for each of the first three harmonics of a sphere with an opening angle of $\varphi_o = 45°$. The properties of the initially-stressed shell considered are E = 300,000 psi,

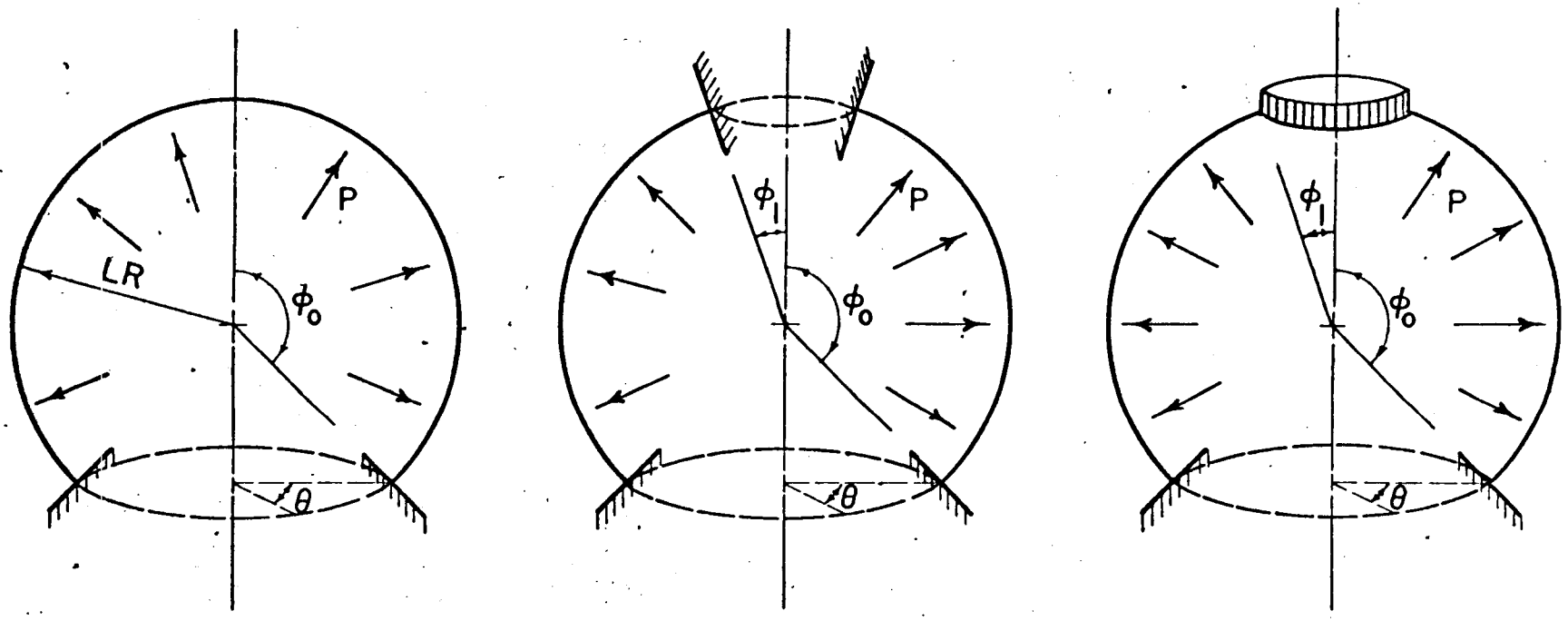

a) CONTINUOUS AT APEX

b) FIXED NEAR APEX

c) RIGID PLUG NEAR APEX

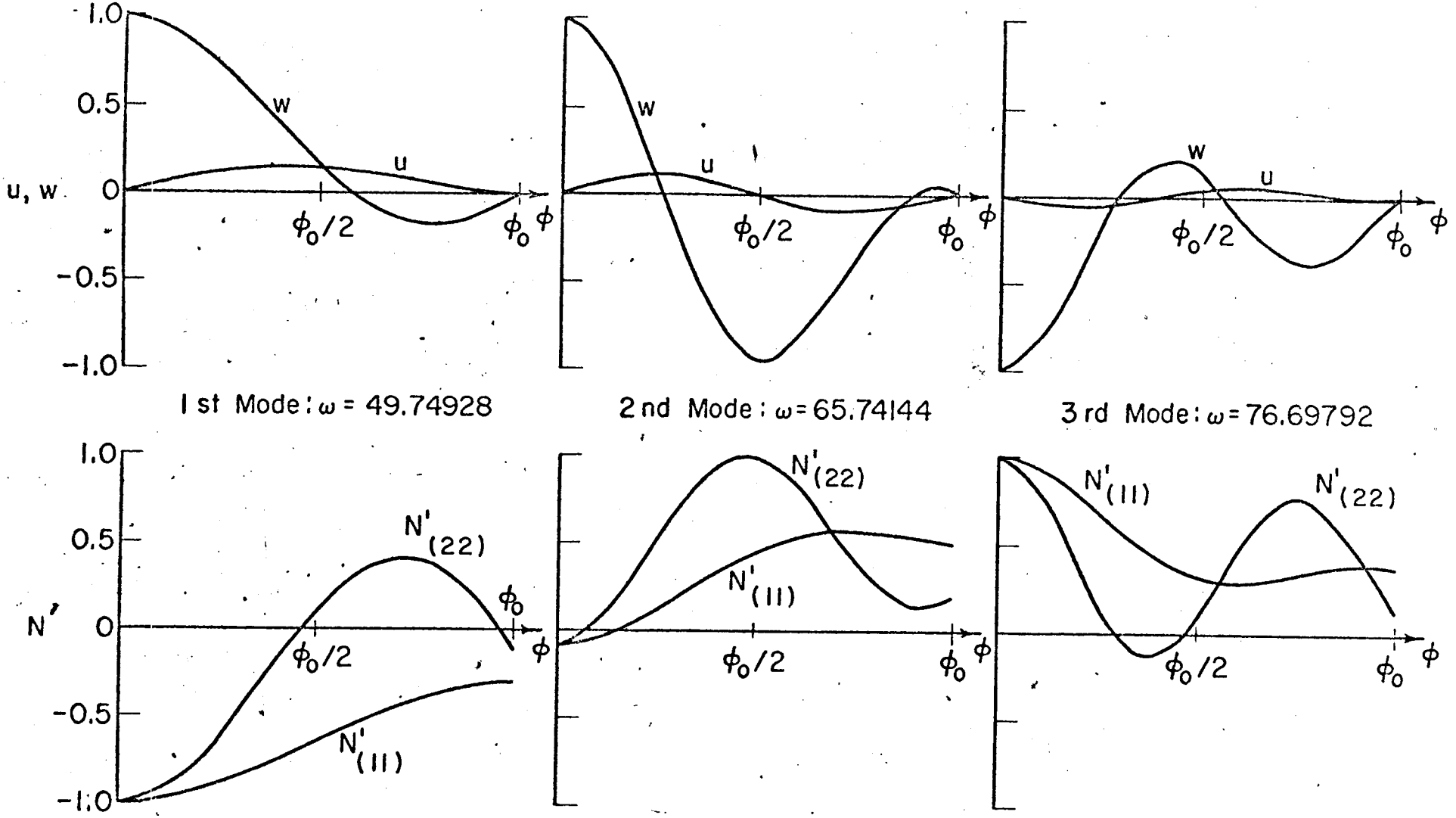
1.0
0.5
0
-0.5
-1.0
u, w
w
u
$\phi_0/2$
ϕ_0
ϕ
1 st Mode : ω = 49.74928
2 nd Mode : ω = 65.74144
3 rd Mode : ω = 76.69792
N'
$N'_{(22)}$
$N'_{(11)}$

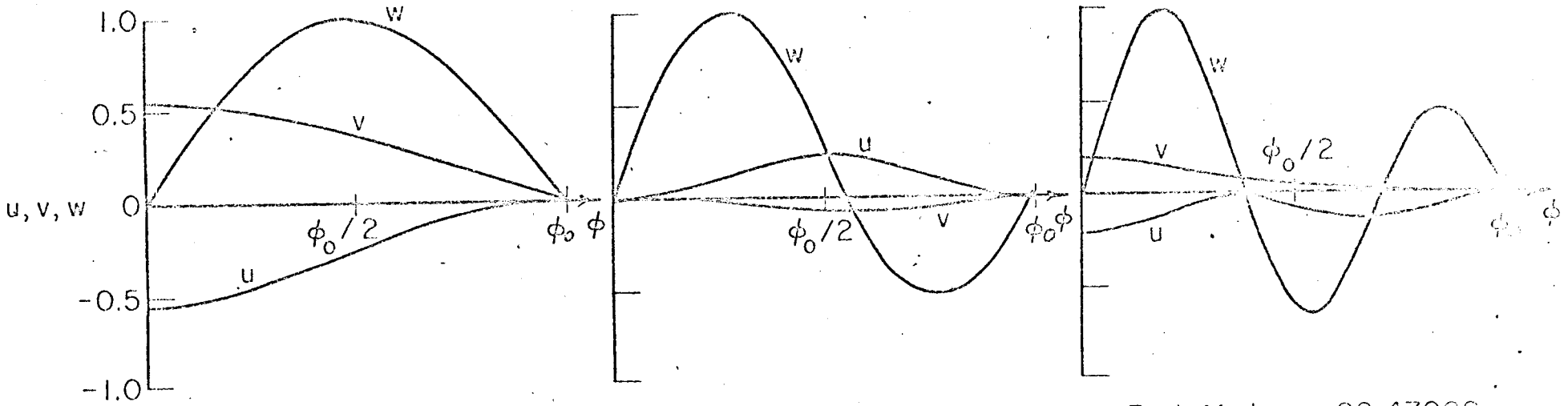

1 st Mode : =44.75748 2 nd Mode : =62.34485 3 rd Mode : =82.47009

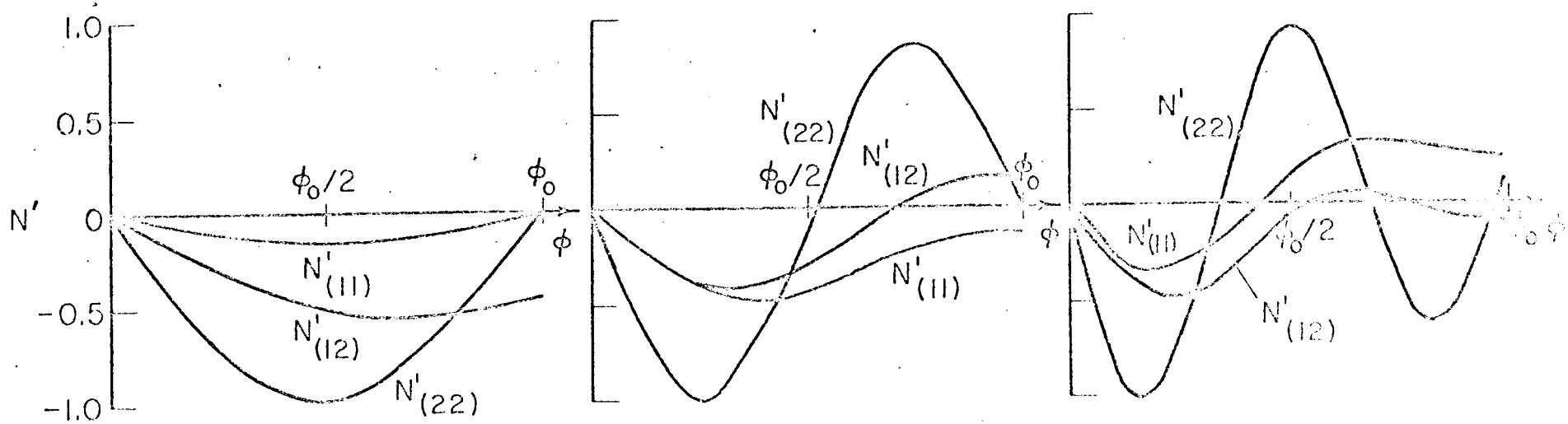

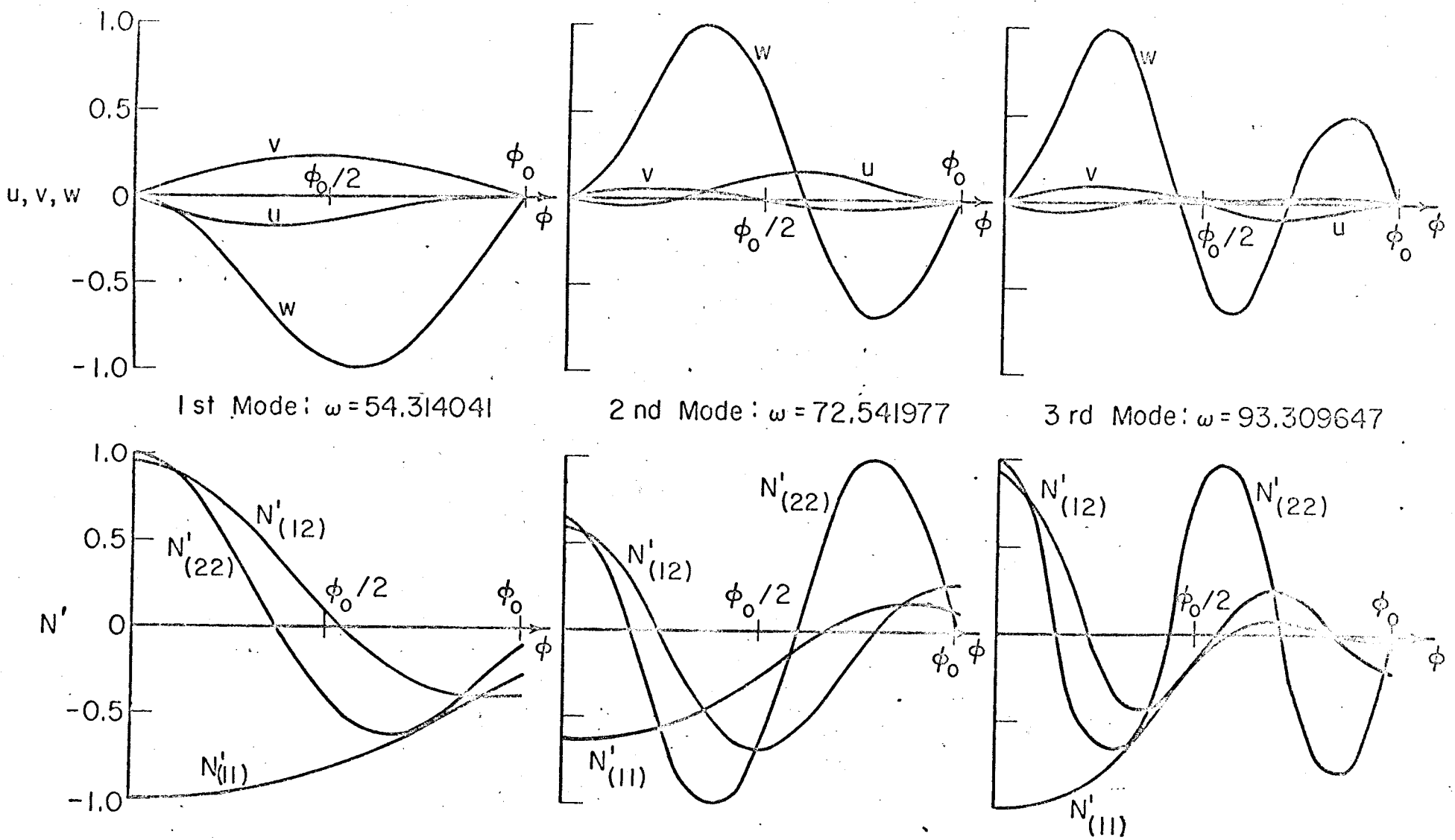
1.0
0.5
u, v, w
0
-0.5
-1.0
v
u
w
$\phi_0/2$
ϕ_0
ϕ
1 st Mode : $\omega = 54.314041$
2 nd Mode : $\omega = 72.541977$
3 rd Mode : $\omega = 93.309647$
N'
$N'_{(12)}$
$N'_{(22)}$
$N'_{(11)}$

$\nu = 0.4$, $\lambda = 0.0001$, L = 100 ft., R = 1, $N_{(11)} = N_{(22)} = 20{,}000$ psf. Figs 6, 7, and 8 show the displacement mode shapes of a hemisphere with these same properties except that $\omega_o = 90°$.

In all of the above examples the exact formulation was used as the basis of solution. When the approximate formulation was used, results were obtained which were in close agreement to the more exact solutions. The solutions for the two formulations are compared in Table 1 for a sphere with an opening angle of 45°.

It is of interest to note that for a steep shell vibrating in its lowest axisymmetric mode there exists a node, w = 0, at an interior point. The location of the node varies with the opening angle considered. Therefore, a uniform, dynamic pressure loading cannot be adequately represented by only one mode when the modal analysis method for forced vibrations (described in a following section) is used. In Fig. 9 are plotted the normal displacements for the first axisymmetric mode shapes of spheres with various opening angles. For extremely steep shells, note that the node occurs near $\omega_o/2$.

The effects of the thickness and initial-stress parameters were also studied. For a shell of constant thickness, both the thickness parameter λ and the initial-stress parameter $N_{(11)}$ are contained within the single parametric expression

$$K_1 = \frac{N_{(11)}\,(1-\nu^2)}{2E\lambda L} \qquad (20)$$

Therefore, for a given initial stress, the effect of a change in thickness can be obtained by maintaining a constant thickness and changing the initial stress. Fig. 10 shows the effect of initial stress on the values of the natural frequencies of a sphere with an opening angle of 45°. It was also found that the initial stress had no appreciable effect on the shapes of the natural modes.

Sphere with Other Boundary Conditions. - Two other sphere problems were considered: 1) a sphere fixed near the apex and at the base, Fig. 2b; and

TABLE 1

COMPARISON OF EXACT AND APPROXIMATE FORMULATIONS FOR A SPHERE CONTINUOUS AT THE APEX AND FIXED AT $\theta_0 = 45°$

	n = 0				n = 1				n = 2			
θ, in degrees	V(exact)	V(approx)	$N'_{(11)}$(exact)	$N'_{(11)}$(approx)	W(exact)	W(approx)	$N'_{(11)}$(exact)	$N'_{(11)}$(approx)	W(exact)	W(approx)	$N'_{(11)}$(exact)	$N'_{(11)}$(approx)
	ω_1(exact) = 49.75		ω_1(approx) = 49.13		ω_1(exact) = 44.76		ω_1(approx) = 43.93		ω_1(exact) = 54.31		ω_1(approx) = 53.45	
0	1.000	1.000	-100.0	-100.0	0.000	0.000	- 0.0	- 0.0	0.000	0.000	100.0	100.0
9	0.815	0.815	- 93.1	- 93.8	0.611	0.609	-56.8	-55.7	0.267	0.266	98.0	96.8
18	0.383	0.382	- 75.7	- 77.7	0.967	0.965	-93.5	-92.5	0.785	0.784	90.0	86.5
27	-0.028	-0.030	- 54.6	- 57.6	0.930	0.930	-97.5	-97.6	0.993	0.993	74.1	69.5
36	-0.175	-0.176	- 37.4	- 40.3	0.541	0.544	-68.5	-69.3	0.627	0.627	51.3	47.8
45	0.000	0.000	- 29.4	- 30.7	0.000	0.000	-16.5	-14.8	0.000	0.000	27.2	26.0
	ω_2(exact) = 65.74		ω_2(approx) = 65.43		ω_2(exact) = 62.34		ω_2(approx) = 61.76		ω_2(exact) = 72.54		ω_2(approx) = 72.05	
0	-1.000	1.000	- 14.3	- 12.3	0.000	0.000	- 0.0	- 0.0	0.000	0.000	-100.0	-100.0
9	0.337	0.338	8.8	8.6	0.922	0.920	-75.0	-71.2	0.575	0.575	-94.7	-90.2
18	-0.730	-0.722	57.6	54.2	0.745	0.747	-100.0	-100.0	0.965	0.968	-66.0	-59.0
27	-0.837	-0.818	93.1	90.5	-0.166	-0.160	-73.0	-80.7	0.022	0.024	-13.5	-14.2
36	-0.185	-0.168	99.0	99.5	-0.546	-0.542	-35.8	-45.2	-0.687	-0.685	23.8	16.9
45	-0.000	-0.000	90.0	91.0	0.000	0.000	-26.0	-29.3	0.000	0.000	17.1	15.1
	ω_3(exact) = 76.69		ω_3(approx) = 76.43		ω_3(exact) = 82.47		ω_3(approx) = 82.02		ω_3(exact) = 93.09		ω_3(approx) = 93.00	
0	-1.000	-1.000	100.0	100.0	0.000	0.000	0.0	0.0	0.000	0.000	-100.0	-100.0
9	-0.415	-0.414	79.5	81.5	0.970	0.990	-82.0	-75.2	0.860	0.859	- 89.6	- 85.5
18	0.211	0.205	44.0	47.5	-0.155	-0.155	-21.5	-21.5	0.346	0.347	- 43.1	- 41.5
27	-0.127	-0.135	30.8	32.4	-0.528	-0.532	85.0	78.0	-0.6336	-0.637	4.5	1.6
36	-0.382	-0.383	36.7	37.4	0.376	0.373	92.2	94.8	0.424	0.421	4.5	7.5
45	0.000	0.000	37.9	40.3	0.000	0.000	73.5	73.6	0.000	0.000	1.6	2.8

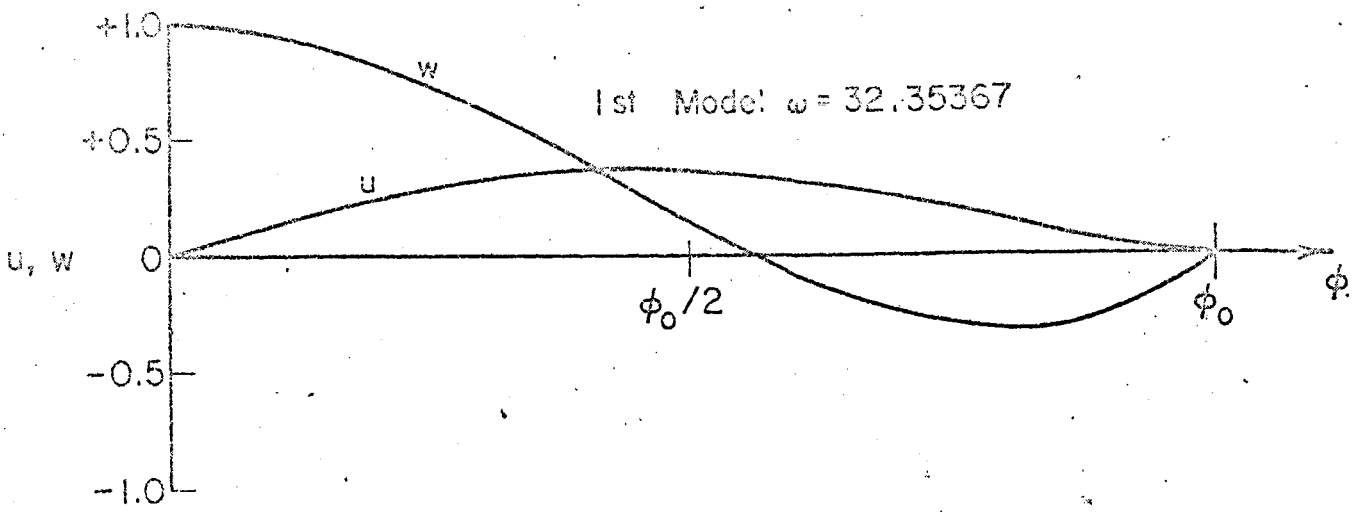
+1.0
+0.5
0
-0.5
-1.0
u, w
w
u
1st Mode: ω = 32.35367
φ0/2
φ0
φ

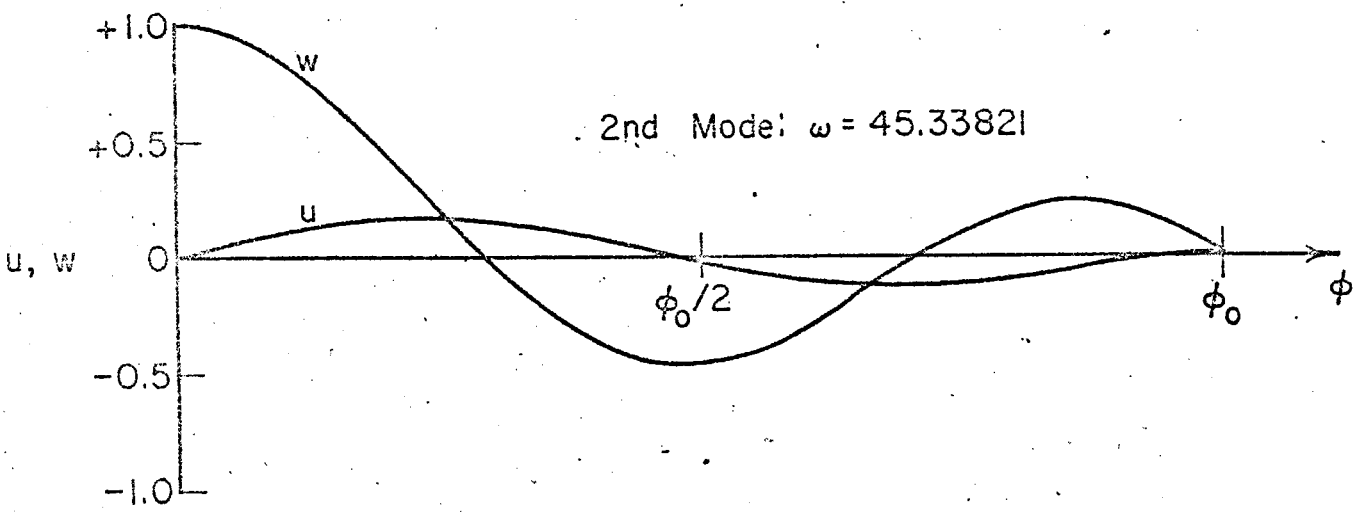
+1.0
+0.5
0
-0.5
-1.0
u, w
w
u
2nd Mode: ω = 45.33821
φ0/2
φ0
φ

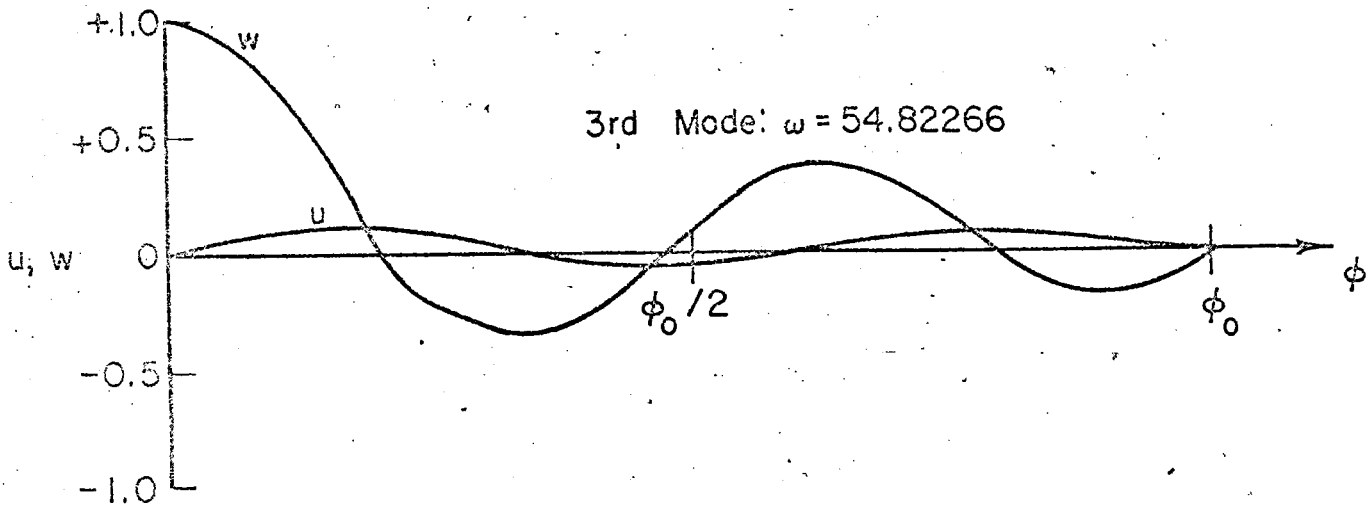
+1.0
+0.5
0
-0.5
-1.0
u, w
w
u
3rd Mode: ω = 54.82266
φ0/2
φ0
φ

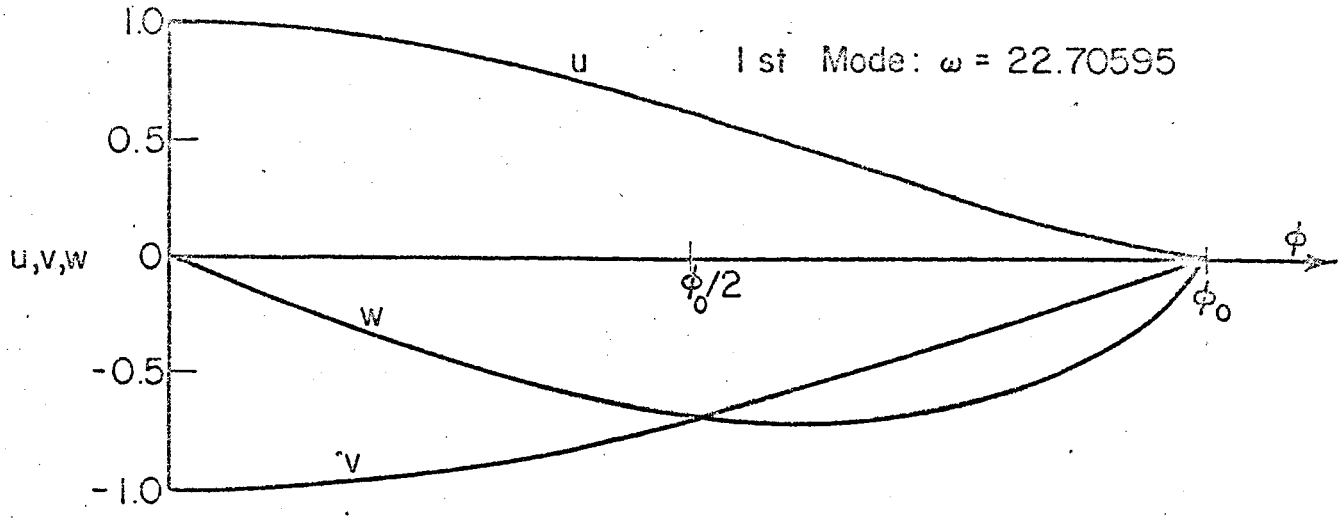
1.0
0.5
u,v,w
0
-0.5
-1.0
u
1 st Mode : ω = 22.70595
w
v
φ
φ0/2
φ0

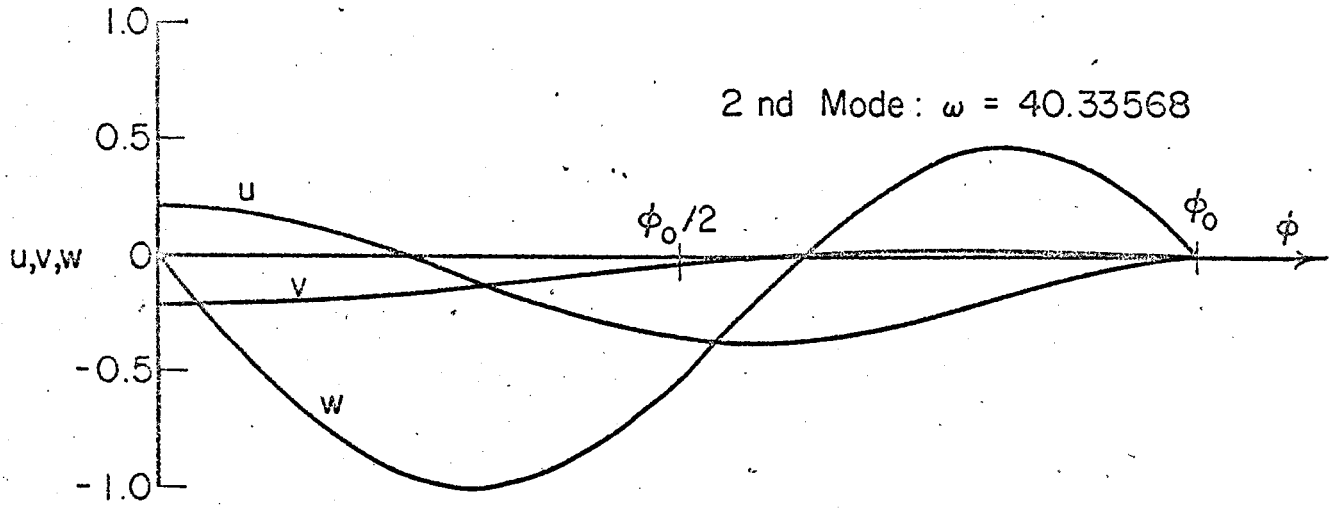
1.0
0.5
u,v,w
0
-0.5
-1.0
2 nd Mode : ω = 40.33568
u
v
w
φ0/2
φ0
φ

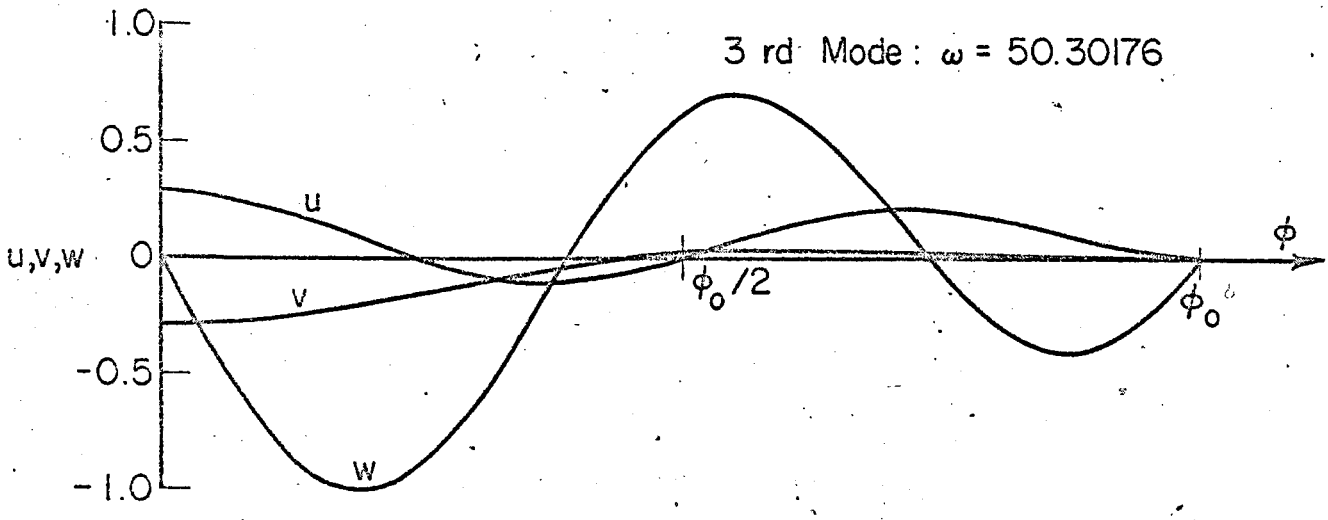
1.0
0.5
u,v,w
0
-0.5
-1.0
3 rd Mode : ω = 50.30176
u
v
w
φ0/2
φ0
φ

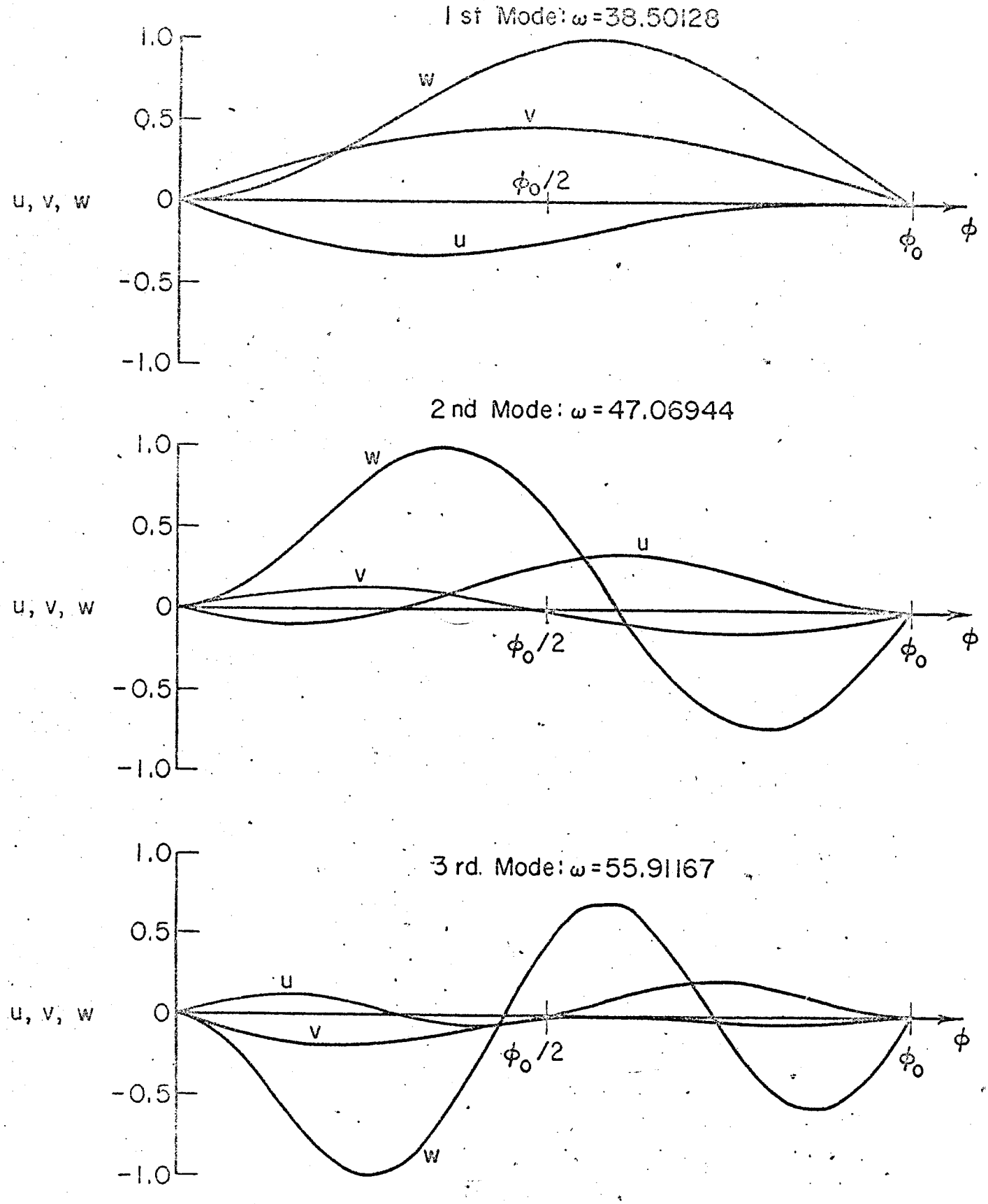
1 st Mode: ω = 38.50128
2 nd Mode: ω = 47.06944
3 rd. Mode: ω = 55.91167
u, v, w
1.0
0.5
0
-0.5
-1.0
w
v
u
φ0/2
φ0
φ

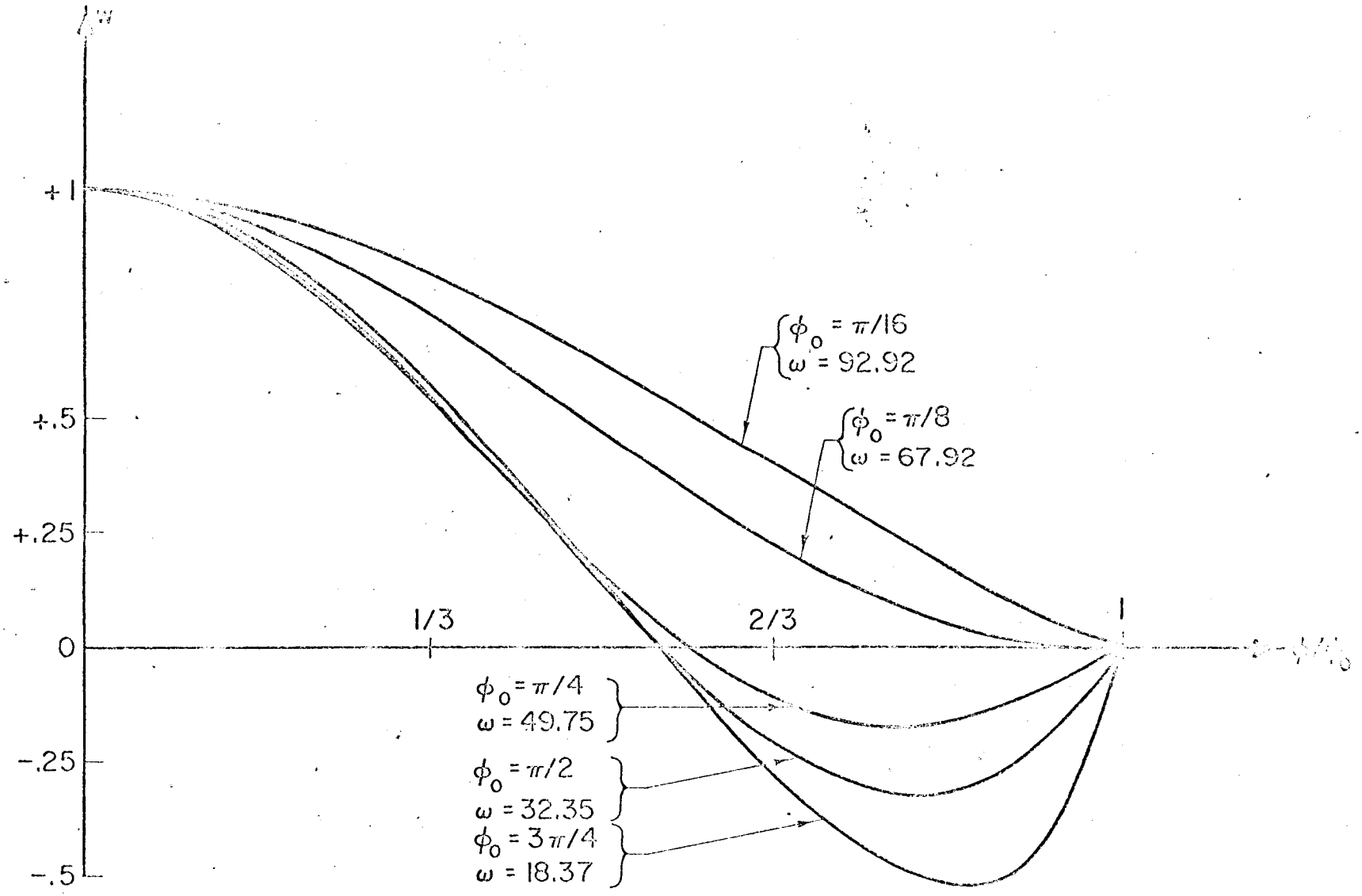
f/w
+1
+.5
+.25
0
-.25
-.5
1/3
2/3
1
x/x0
$\phi_0 = \pi/16$
$\omega = 92.92$
$\phi_0 = \pi/8$
$\omega = 67.92$
$\phi_0 = \pi/4$
$\omega = 49.75$
$\phi_0 = \pi/2$
$\omega = 32.35$
$\phi_0 = 3\pi/4$
$\omega = 18.37$

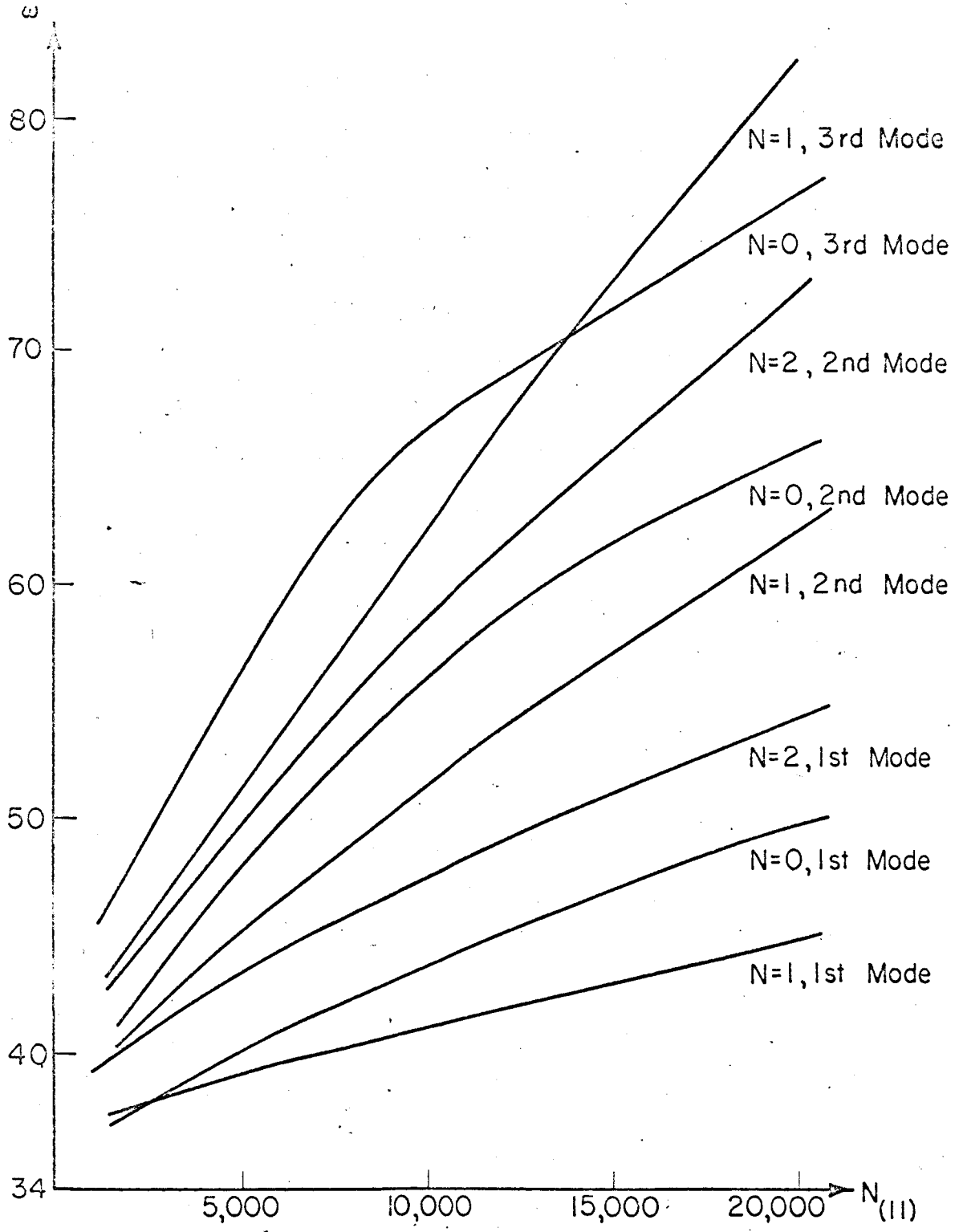
ω
80
70
60
50
40
34
N=1, 3rd Mode
N=0, 3rd Mode
N=2, 2nd Mode
N=0, 2nd Mode
N=1, 2nd Mode
N=2, 1st Mode
N=0, 1st Mode
N=1, 1st Mode
5,000
10,000
15,000
20,000
N(11)

2) a sphere with a rigid plug near the apex and fixed or simply-supported at the base, Fig. 2c. Several numerical problems were considered. Fig. 11 shows the first three normal displacement mode shapes for the first three harmonics of two sphere problems with $\varphi_o = 45°$. In both examples the shell near the apex is assumed to be attached to the fixed support and to the rigid plug, respectively, at $\varphi = 1°$.

The initial-stress states for these two examples were obtained via uniform internal pressure. In the case of a sphere fixed at both ends of the meridian, it was assumed that the sphere was completely supported on rollers which, after the desired configuration was obtained, were rigidly clamped. The initial-stress resultants for a fixed-fixed sphere therefore are the same as those used in the previous section for a sphere continuous at the apex. In a similar fashion for the sphere with a rigid plug near the apex, it was assumed that the sphere boundary conditions during the pressurization phase were that the base was on roller supports and that near the apex the sphere was attached to a rigid plug. After pressurization, the sphere is then completely clamped at the base. The initial-stress resultants for a sphere with a rigid plug near the apex are therefore

$$N_{(11)} = \frac{\bar{p}LR}{2\sin^2\varphi}\left[\sin^2\varphi + \frac{1-\nu}{1+\nu}\sin^2\varphi_1\right] \tag{21a}$$

$$N_{(22)} = \frac{\bar{p}LR}{2\sin^2\varphi}\left[\sin^2\varphi - \frac{1-\nu}{1+\nu}\sin^2\varphi_1\right] \tag{21b}$$

where the solutions have been linearized, i.e. terms of order $\frac{\bar{p}^2L}{\lambda E}$ have been neglected, and where φ_1 = angular location of rigid plug.

Shells of Revolution with More Complex Geometries. - In order to demonstrate the solution procedure on a sample problem with a more complex geometry then that of a sphere, two further examples were considered: 1) the paraboloid of revolution shown in Fig. 12, and 2) the toroidal section shown in Fig. 13. For the paraboloid of revolution, several numerical examples were solved. The

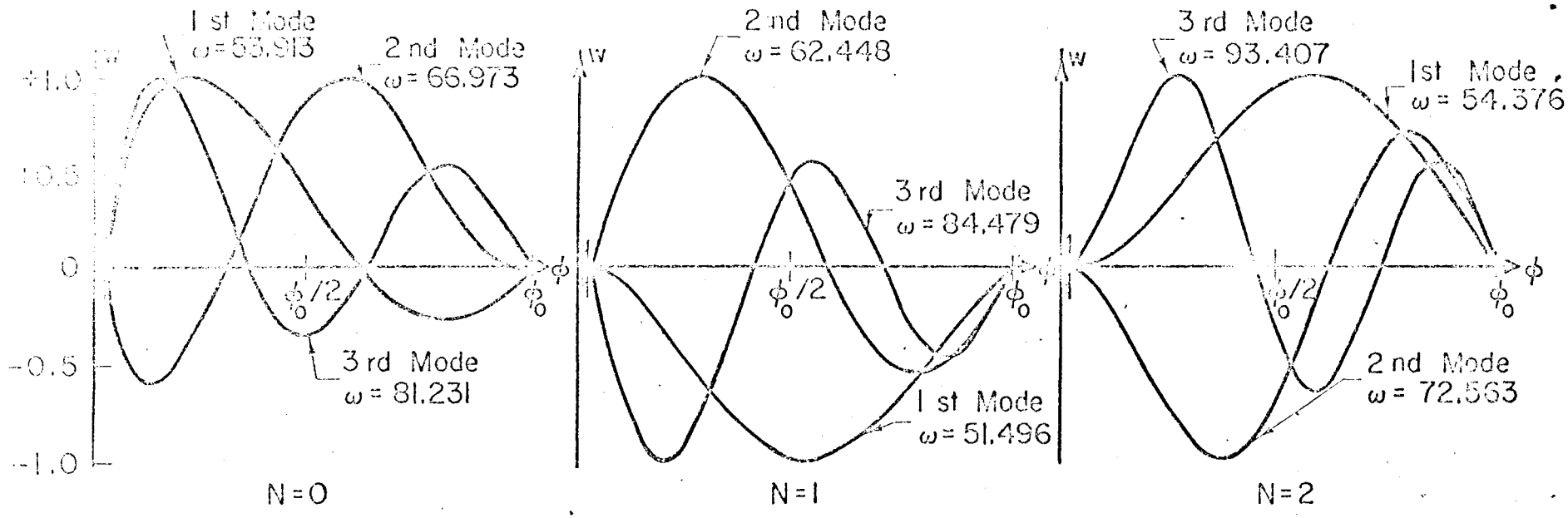

FIXED NEAR APEX, FIXED AT $\phi_0 = 45°$

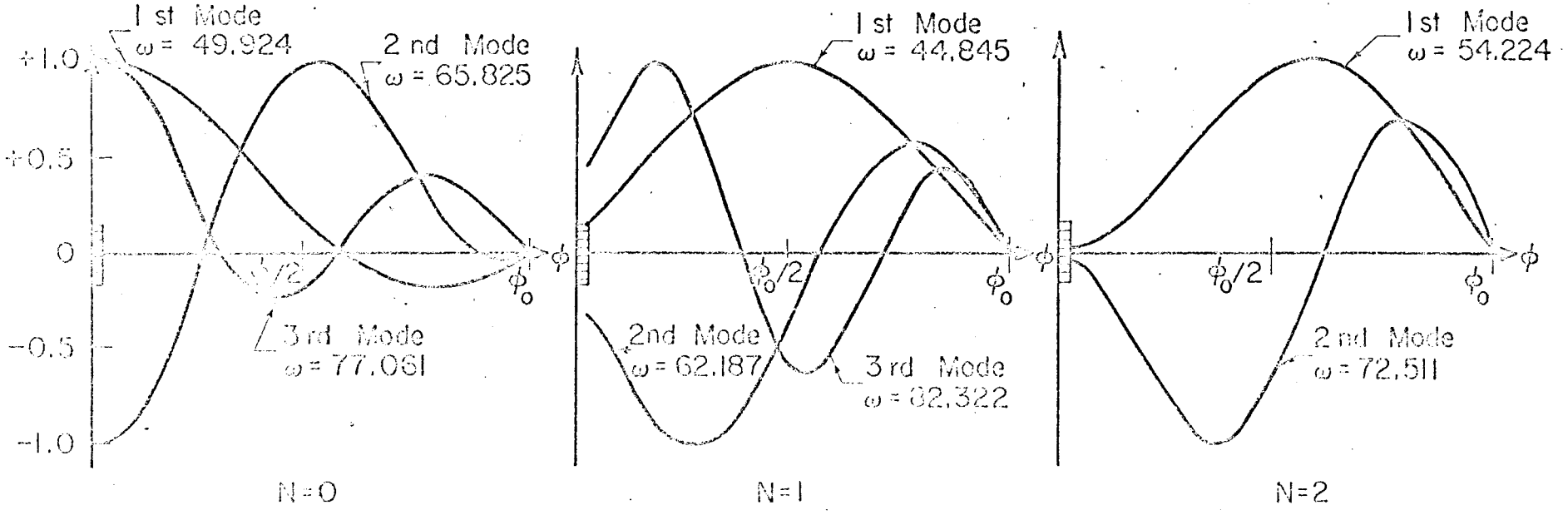

RIGID PLUG NEAR APEX, FIXED AT $\phi_0 = 45°$

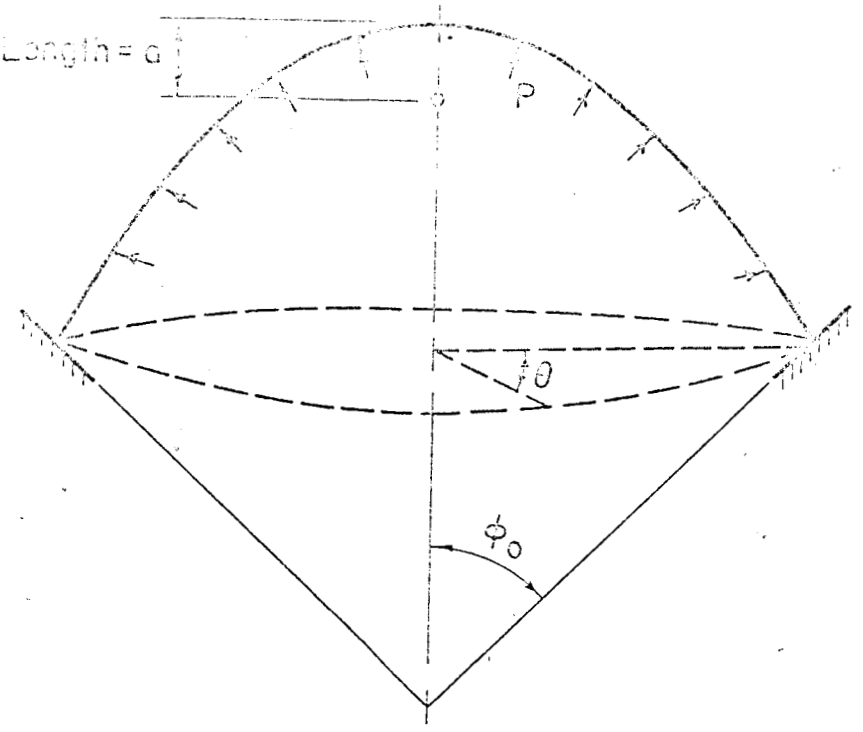
Focal Length = a
P
θ
φo

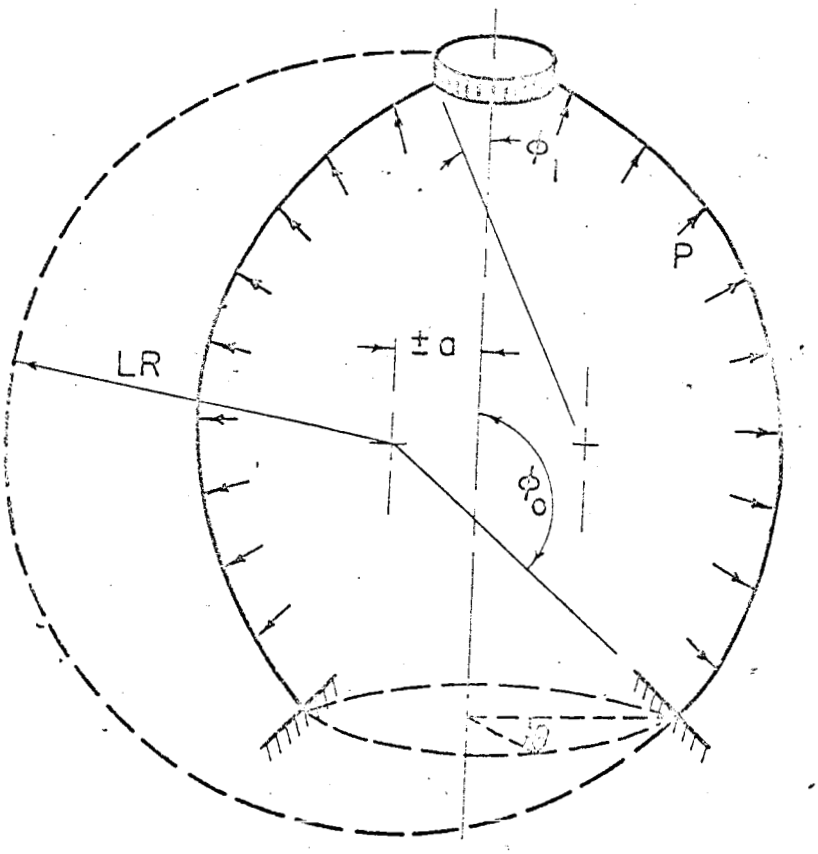
φi
P
LR
±a
φo

results of one of these problems are depicted in Fig. 14, where the first three displacement mode shapes are plotted for the first two harmonics of a paraboloid continuous at the apex and fixed at $\varphi_o = 45°$. The data for the particular paraboloid considered in Fig. 14 is E = 300,000 psi, $\nu = 0.4$, $\lambda = 0.0001$, L = 50 ft., a = 1, $\bar{p}$ = 500 psf, where $\bar{p}$ is the internal pressure used to calculate the initial-stress resultants (18).

The toroidal shell problem considered, Fig. 13, was that of a section of a torus fixed at the base, $\varphi = \varphi_o$, and attached to a rigid plug near the apex. The numerical data for the particular example considered are E = 300,000 psi, $\nu = 0.4$, L = 100 ft., a = -0.25, $\varphi_1 = 30°$, $\varphi_o = 90°$, and $\bar{p}$ = 400 psf, where $\bar{p}$ is the internal pressure used in the calculation of the initial-stress resultants by the following equations

$$N_{(11)} = \frac{L\bar{R}\bar{p}}{(a + R \sin\varphi)} \left\{a + \frac{R \sin\varphi}{2}\left[1 + \frac{\sin^2\varphi}{\sin^2\varphi_1} \frac{a(1-2\nu) + R(1-\nu)\sin\varphi_1}{a + R(1+\nu)\sin\varphi_1}\right]\right\} \quad (22a)$$

$$N_{(22)} = \frac{L\bar{R}\bar{p}}{2}\left\{1 - \frac{\sin^2\varphi_1}{\sin^2\varphi} \frac{a(1-2\nu) + R(1-\nu)\sin\varphi_1}{a + R(1+\nu)\sin\varphi_1}\right\} \quad (22b)$$

The first three normal displacement mode shapes for the first three harmonics of this particular example are shown in Fig. 15.

FORCED VIBRATIONS

Once the natural frequencies and associated mode shapes of free vibration for a thin initially-stressed shell of revolution have been obtained, it is possible to determine the response of the shell to time-dependent loading conditions by means of the modal analysis method (3, 13, 17, 31). In this method it is assumed the transient displacements can be represented as an infinite, convergent sum of the mode shapes of free vibration, each mode shape being multiplied by a time dependent participation factor. The problem is then reduced to the determination of a sufficient number of mode participation factors to

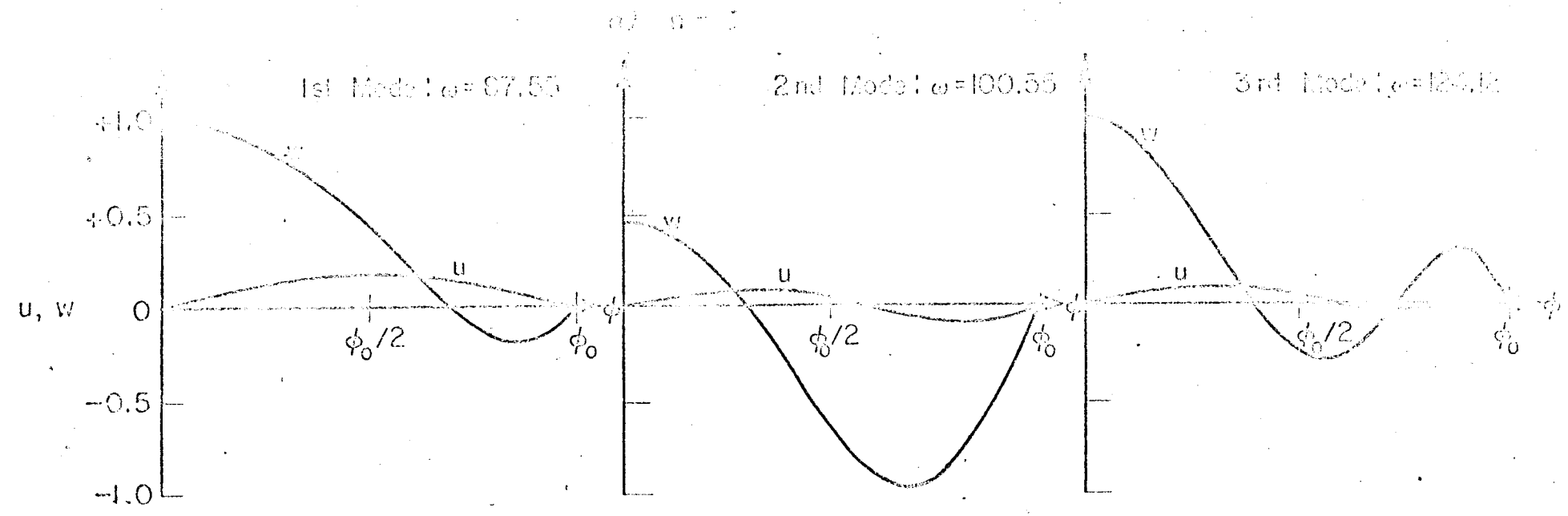
1st Mode : ω = 97.55
2nd Mode : ω = 100.55
3rd Mode : ω = 126.8
+1.0
+0.5
u, w
0
-0.5
-1.0
u
w
φ0/2
φ0
φ

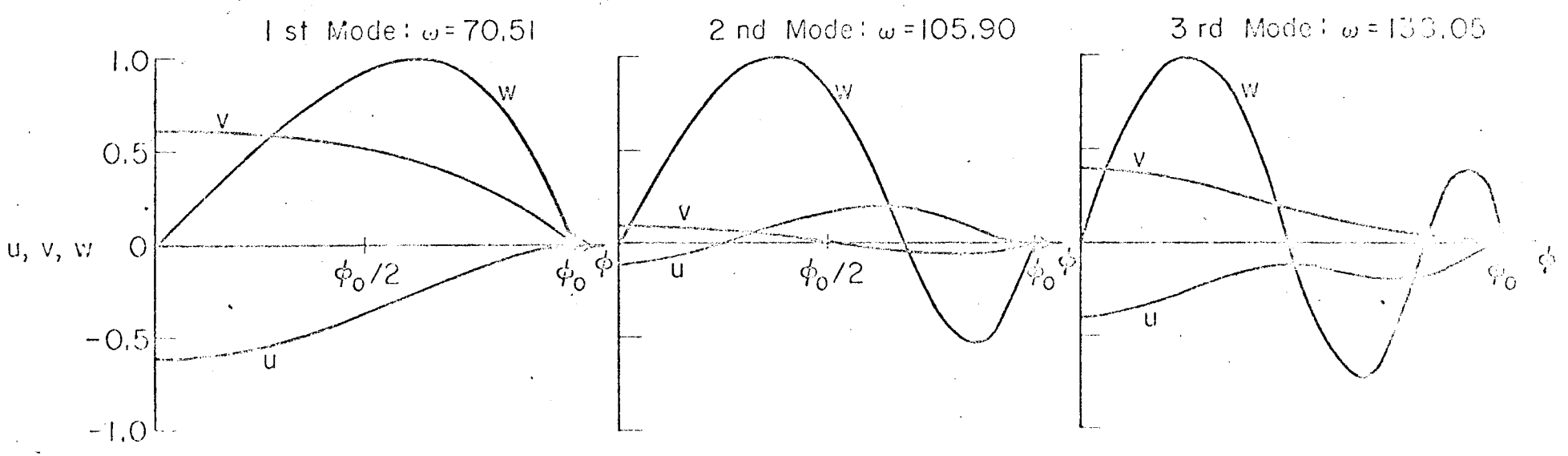
1 st Mode : ω = 70.51
2 nd Mode : ω = 105.90
3 rd Mode : ω = 133.05
1.0
0.5
u, v, w
0
-0.5
-1.0
v
w
u
φ0/2
φ0
φ

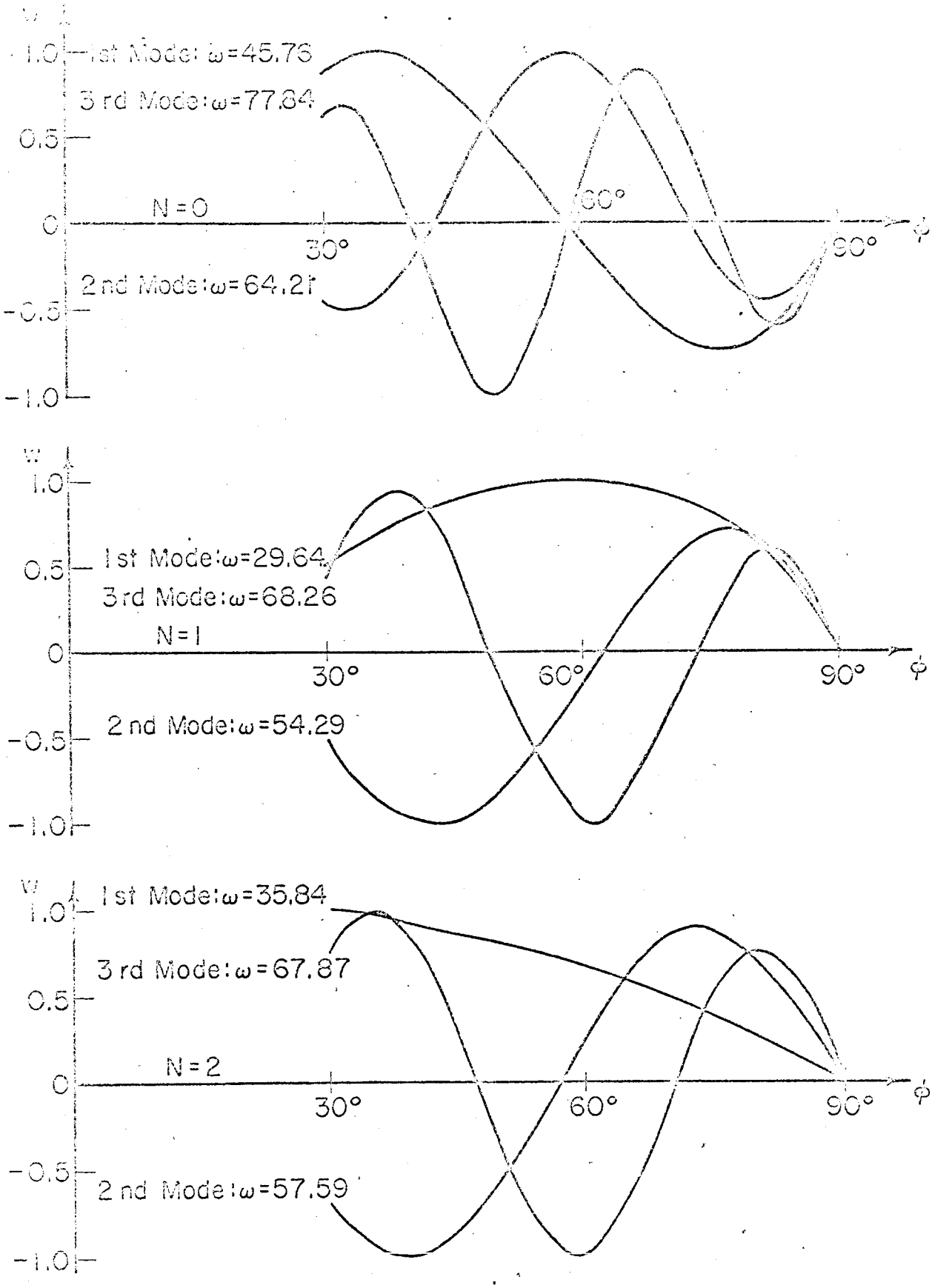
W
1.0
1st Mode: ω=45.76
3rd Mode: ω=77.84
0.5
N=0
0
30°
60°
90°
Φ
2nd Mode: ω=64.21
-0.5
-1.0
W
1.0
0.5
1st Mode: ω=29.64
3rd Mode: ω=68.26
N=1
0
30°
60°
90°
Φ
2nd Mode: ω=54.29
-0.5
-1.0
W
1.0
1st Mode: ω=35.84
3rd Mode: ω=67.87
0.5
N=2
0
30°
60°
90°
Φ
-0.5
2nd Mode: ω=57.59
-1.0

adequately represent the forced response of the initially-stressed shell.

The equations of motion can be written as

$$L_1(u, v, w) + LP'_{(1)}\sqrt{A}_{11} - 2\lambda\rho L^3 \sqrt{A}_{11} \frac{\partial^2 u}{\partial t^2} - 2\lambda C L^3 \sqrt{A}_{11} \frac{\partial u}{\partial t} = 0 \tag{23a}$$

$$L_2(u, v, w) + LP'_{(2)}r - 2\lambda\rho L^3 r \frac{\partial^2 v}{\partial t^2} - 2\lambda C L^3 r \frac{\partial v}{\partial t} = 0 \tag{23b}$$

$$L_3(u, v, w) + LP'_{(3)} - 2\lambda\rho L^3 \frac{\partial^2 w}{\partial t^2} - 2\lambda C L^3 \frac{\partial w}{\partial t} = 0 \tag{23c}$$

where $L_i(u, v, w)$ = differential operator related to the equivalent static problem, and C = coefficient of viscous damping. Note that Eqs. 23 are a slight generalization of Eqs. 7 or 8 in that a first approximation to the effect of viscous damping has been included. It is assumed that the shell is underdamped, i.e. $C < C_{cr}$, where C_{cr} is the coefficient of critical damping.

Let the displacements be expanded in terms of the natural modes as follows

$$u(x^1, \theta, t) = \sum_{n=0}^{\infty} \sum_{i=1}^{\infty} u^n_i (x^1) \cos n\theta \, F_{ni}(t) \tag{24a}$$

$$v(x^1, \theta, t) = \sum_{n=1}^{\infty} \sum_{i=1}^{\infty} v^n_i (x^1) \sin n\theta \, F_{ni}(t) \tag{24b}$$

$$w(x^1, \theta, t) = \sum_{n=0}^{\infty} \sum_{i=1}^{\infty} w^n_i (x^1) \cos n\theta \, F_{ni}(t) \tag{24c}$$

where u^n_i, v^n_i, w^n_i are the modal displacements for the i^{th} ordered mode of the n^{th} harmonic, and $F_{ni}(t)$ is the corresponding time-dependent mode participation factor.

The Equations 23 are combined as follows: 1) Eqs. 24 are substituted into Eqs. 23; 2) the equations of motion for free vibration are used to eliminate each of the L_i's; 3) the equations are multiplied by $u^n_i \cos n\theta$, $v^n_i \sin n\theta$, $w^n_i \cos n\theta$ respectively and then added together; 4) the result is then integrated over the surface area of the initially-stressed middle surface; and 5) orthogonality properties of the natural modes are used to eliminate terms. When the above steps are completed, the following ordinary differential equation is obtained

$$\ddot{F}_{ni} + 2\omega_{ni}\beta \dot{F}_{ni} + F_{ni} = Q_{ni}(t) \tag{25a}$$

where

$$Q_{ni}(t) = \frac{1}{2\rho L^3 K_{ni}} \int_a^b \left[u_i^n P'^n_{(1)} + v_i^n P'^n_{(2)} + w_i^n P'^n_{(3)}\right] \frac{r\sqrt{A_{11}}}{\lambda} dx^1 \tag{25b}$$

$$K_{ni} = \int_a^b \left[(u_i^n)^2 + (v_i^n)^2 + (w_i^n)^2\right] r\sqrt{A_{11}}\, dx^1 \tag{25c}$$

In the above equations, $F_{ni} = dF_{ni}/dt$, ω_{ni} is the i^{th} ordered natural frequency for the n^{th} harmonic, β is ratio of the coefficient of damping to the coefficient of critical damping, K_{ni} is the modal normalization constant, and $P'_{(i)}(x^1, \theta, t)$ have been expanded as Fourier series in θ.

The problem of determining the transient response of initially-stressed shells for which natural frequencies and mode shapes are available has been reduced to that of solving the classical initial-value problem posed by Eqs. 25 for F_{ni}. The initial-value problem can be integrated by means of Duhamel integral techniques if the transient load vector is expressible in terms of a single forcing function, or by means of the generalized Holzer method. The latter was chosen in this study.

Initial Conditions.- It is necessary to prescribe initial conditions for F_{ni} and $\dot{F}_{ni}$ at time $t = 0$. These conditions can be arrived at from consideration of Eqs. 27. The initial condition for the shell displacements and velocities are

$$u(x^1, \theta, 0) = \sum_{n=0}^{\infty} u_o^n (x^1) \cos n\theta \tag{26a}$$

$$v(x^1, \theta, 0) = \sum_{n=1}^{\infty} v_o^n (x^1) \cos n\theta \tag{26b}$$

$$w(x^1, \theta, 0) = \sum_{n=0}^{\infty} w_o^n (x^1) \cos n\theta \tag{26c}$$

If steps 3 through 5 (as outlined above for the equations of motion) are repeated using Eqs. 26, the following initial conditions on $F_{ni}(t)$ are obtained

$$\bar{F}_{ni}(0) = \frac{1}{K_{ni}} \int_a^b (u_o^n u_i^n + v_o^n v_i^n + w_o^n w_i^n)\, r\sqrt{A_{11}}\, dx^1 \tag{27a}$$

$$\dot{\bar{F}}_{ni}(0) = \frac{1}{K_{ni}} \int_a^b (\dot{u}_o^n u_i^n + \dot{v}_o^n v_i^n + \dot{w}_o^n w_i^n)\, r\sqrt{A_{11}}\, dx^1 \tag{27b}$$

In order to treat a particular forced vibration problem, using as a basis for solution the superposition theory presented herein, it is necessary to select a value for ϵ', the small non-dimensional parameter defined by the superposed load vector. If the dynamic load vector superposed is denoted by $_{\Delta}\bar{P}(t)$, a reasonable measure for ϵ' is

$$\epsilon' = \frac{\int_0^{2\pi} \int_a^b {}_{\Delta}\bar{P}_{max}(t)\, r\sqrt{A_{11}}\, dx^1\, d\theta}{\int_0^{2\pi} \int_a^b \bar{F}\, r\sqrt{A_{11}}\, dx^1} \tag{28a}$$

where $\bar{F}$ is the static load vector on the initially-stressed shell.

For transient response problems in which superposed initial displacements and velocitics are considered, a reasonable measure for ϵ' is

$$\epsilon' = \frac{\int_0^{2\pi} \int_a^b \left[{}_{\Delta}\bar{V}(x^1, \theta, 0) + \frac{\dot{\bar{V}}(x^1, \theta, 0)}{\omega_{fund}} \right] r\sqrt{A_{11}}\, dx^1 d\theta}{\int_0^{2\pi} \int_a^b \bar{V}_o(\omega, \theta)\, r\sqrt{A_{11}}\, dx^1 d\theta} \tag{28b}$$

where $_{\Delta}\bar{V}(x^1, \theta, 0)$ and $_{\Delta}\dot{\bar{V}}(x^1, \theta, 0)$ are the superposed initial displacement and velocity vectors, respectively, and where $\bar{V}_o$ is the non-dimensional static displacement vector of the initially-stressed middle surface.

Sample Forced Vibration Problems. - The modal analysis method was tested on several dynamic problems. It is not the purpose of this section to solve a problem of particular interest, but rather to demonstrate the modal analysis method and also to show the validity of the mode shapes found in the previous free vibration sample problems. Therefore, three simple problems were chosen:

1) a crude approximation to a static wind load (7),

$$\epsilon' P'_{(3)} = \epsilon' \bar{p} \sin \varphi \cos \theta \qquad 0 < t < \infty ;$$

2) a constant over-pressure $\epsilon' P'_{(3)} = \epsilon' \bar{p}$; and 3) an initial velocity distribution proportional to the static displacement field of the initially-stressed shell. The first two problems were chosen because the static results of the same problems are available for comparison, thus providing a check on the validity of the free vibration mode shapes. In all three problems, β was chosen (31) as 0.01.

Fig. 16 shows the dynamic wind ($\epsilon' \bar{p}$ = 40 psf) stresses at two meridional points on a sphere continuous at the apex and fixed at $\varphi_o = 45°$. At time t = ∞, the dynamic oscillations have died out and the displacements as calculated by the modal analysis method should equal the displacements as calculated from the static theory (20). In Fig. 17, the first three partial sums (at t = ∞) of the normal modes multiplied by the participation factors are compared to the equivalent static solution. It can be seen that only 3 modes need be considered in order to give answers in close agreement with the static solution.

In Figs. 18 and 19, the partial sums of the displacement and stress mode shapes of a sphere continuous at the apex and fixed at $\varphi_o = 45°$, each mode being multiplied by a limiting participation factor for a constant overpressure of 40 psf, are compared to the equivalent static solution (18). It can be seen that more mode shapes are required to adequately represent the static stresses than are required to represent the static displacements.

The final problem considered was that of the response of a sphere, continuous at the apex and fixed at $\varphi_o = 45°$, to an initial velocity distribution with a shape proportional to the static displacement field of the pressurized sphere. In this case

$$\epsilon' = \frac{\int_0^{2\pi} \int_0^{\varphi_o} \frac{1}{\omega_{fund}} \, c \, \bar{V}_o \, r\sqrt{A_{11}} \, d\varphi d\theta}{\int_0^{2\pi} \int_0^{\varphi_o} \bar{V}_o \, r\sqrt{A_{11}} \, d\varphi d\theta} = \frac{c}{\omega_{fund}} = .06025$$

where c is the constant of proportionality (chosen as 3.0), and from Fig. 3, ω_{fund} = 49.75. The partial sum of 5 modes was found to give an adequate

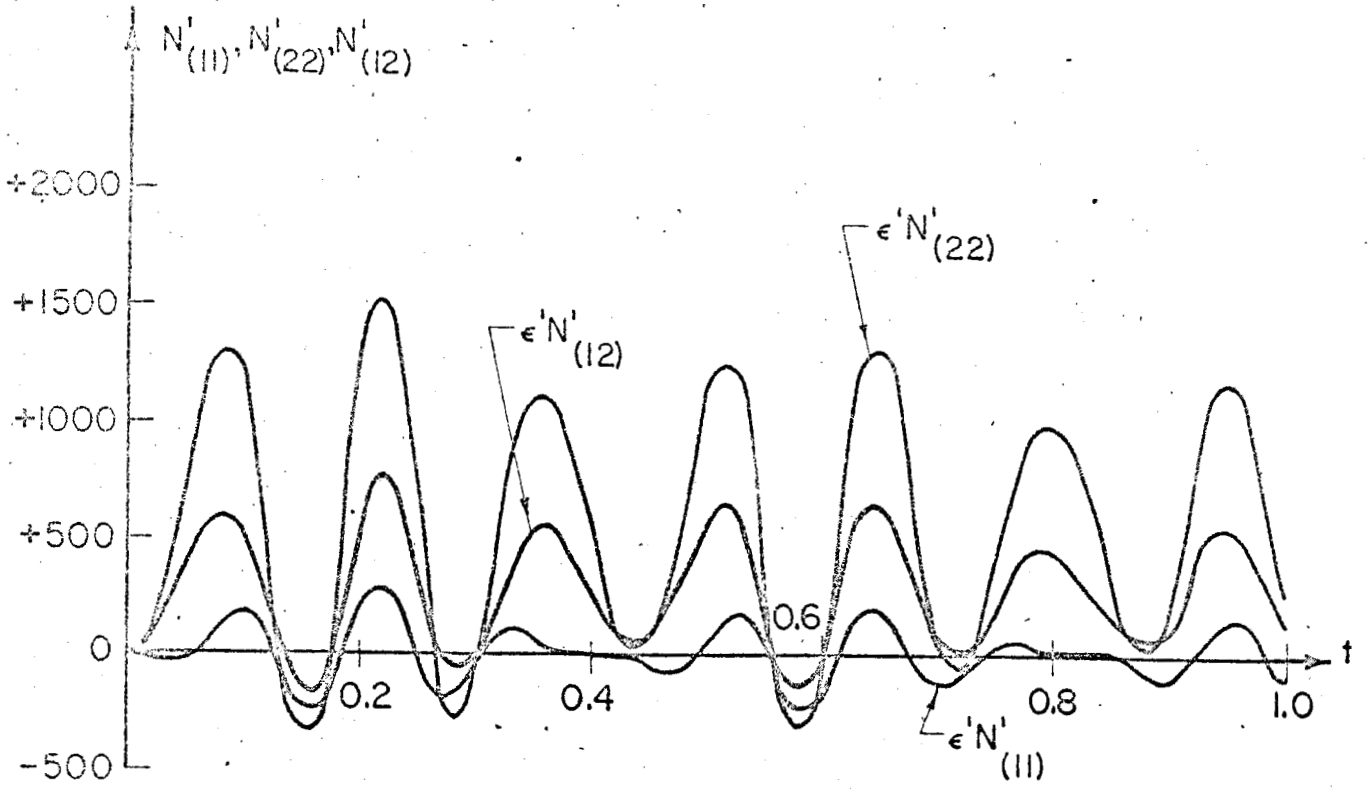

STRESSES AT ϕ = 15°

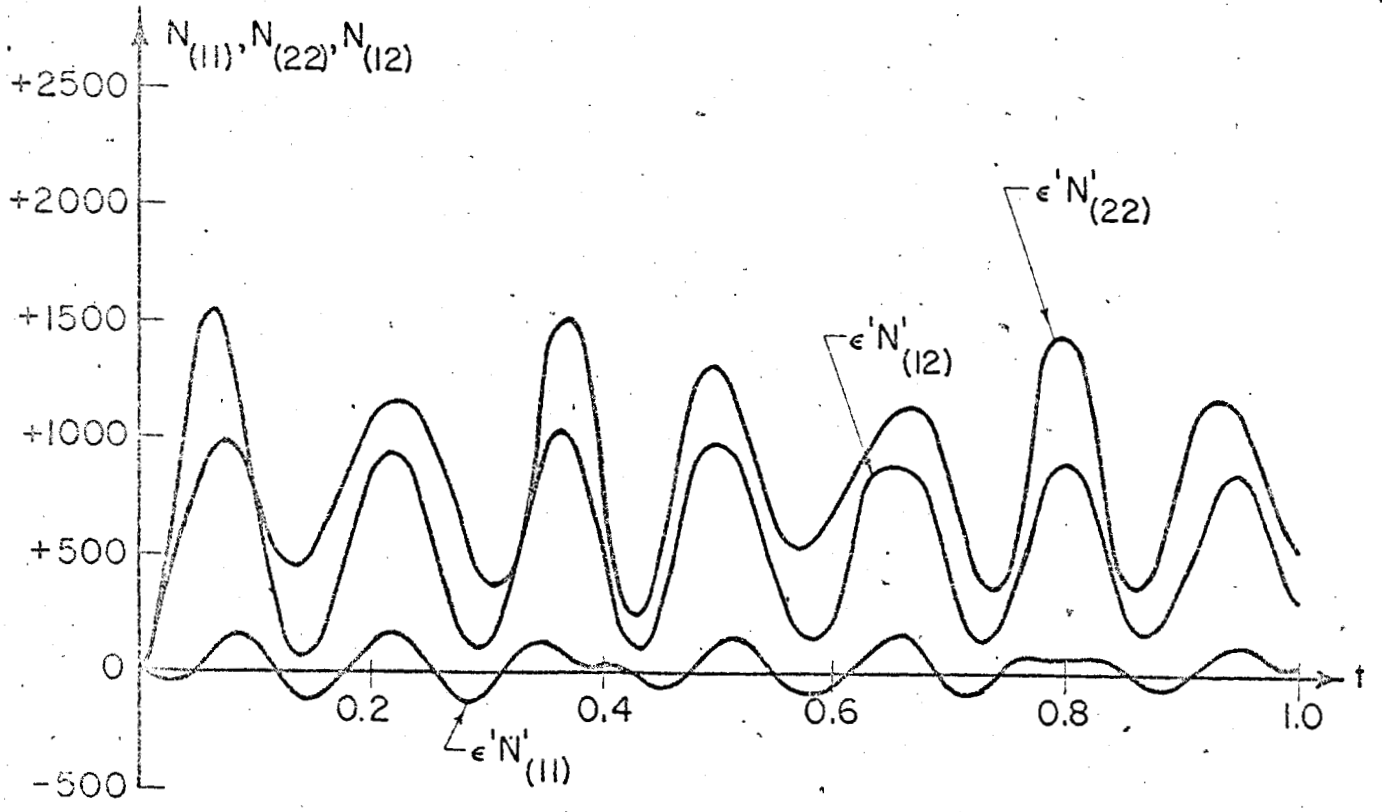

STRESSES AT ϕ = 35°

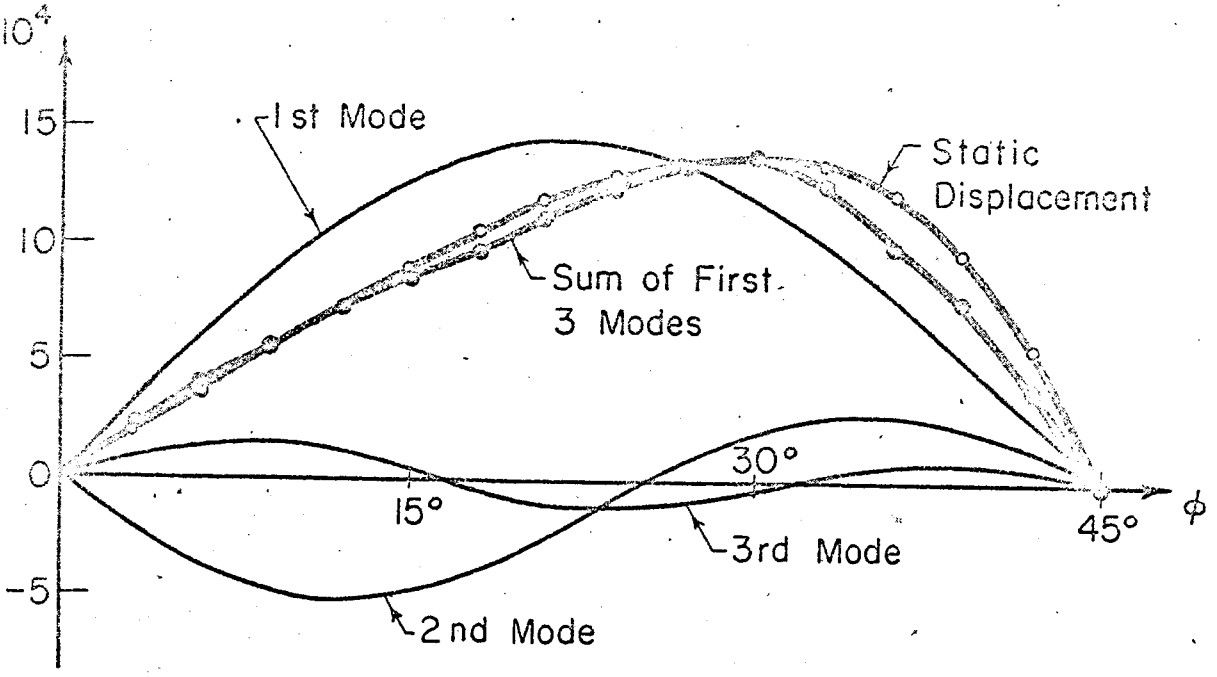
$\epsilon' w' \times 10^4$
15
10
5
0
-5
1st Mode
Static
Displacement
Sum of First
3 Modes
30°
15°
45°
ϕ
3rd Mode
2nd Mode

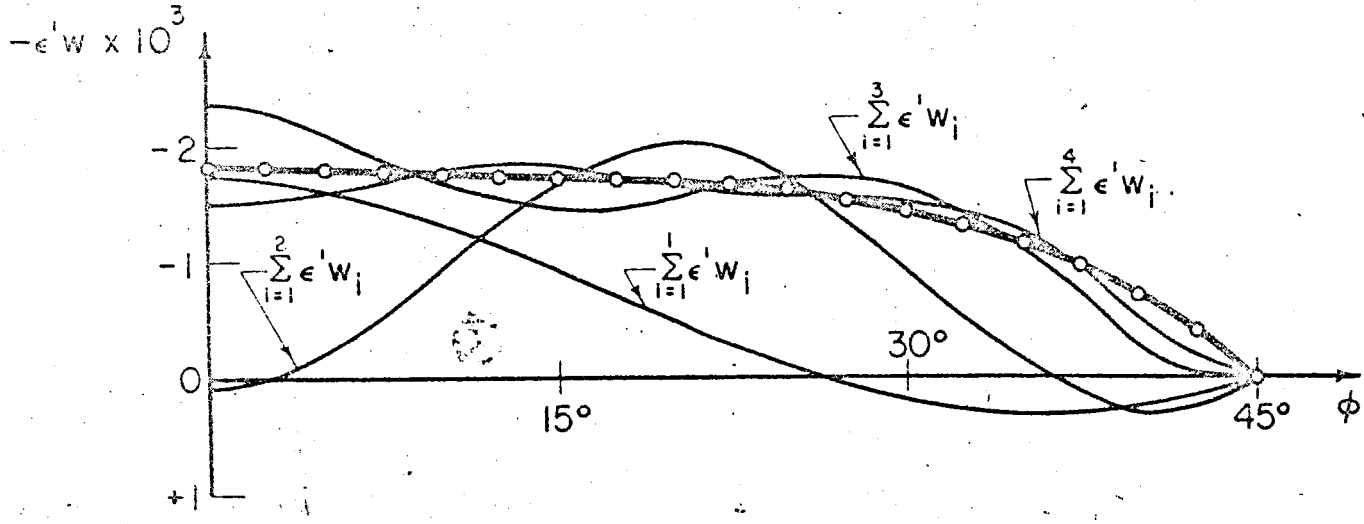
$-\epsilon' w \times 10^3$
-2
-1
0
+1
$\sum_{i=1}^{3} \epsilon' w_i$
$\sum_{i=1}^{4} \epsilon' w_i$
$\sum_{i=1}^{2} \epsilon' w_i$
$\sum_{i=1}^{1} \epsilon' w_i$
30°
15°
45°
ϕ

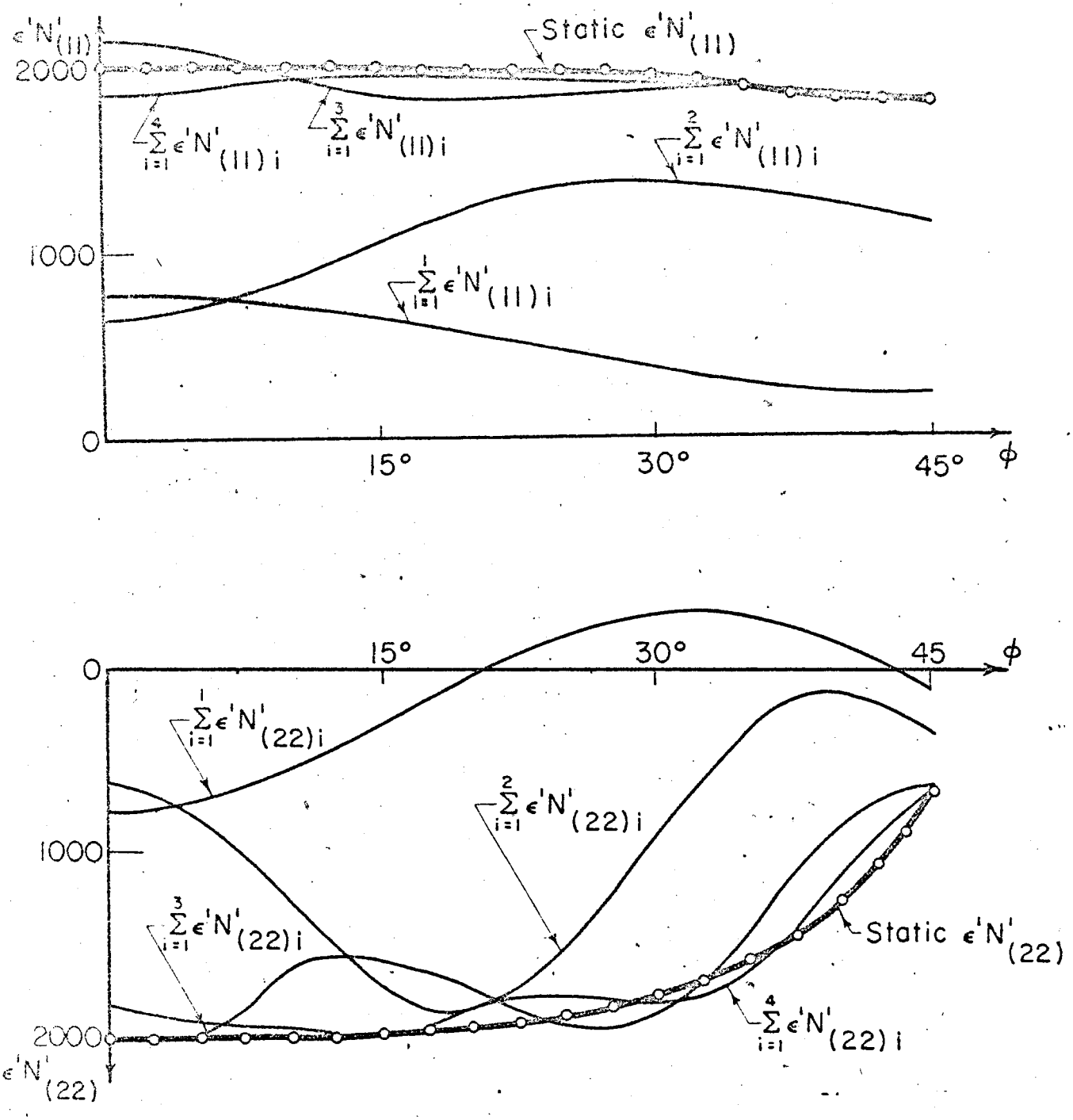
$\epsilon' N'_{(11)}$
2000
1000
0
Static $\epsilon' N'_{(11)}$
$\sum_{i=1}^{4} \epsilon' N'_{(11)i}$
$\sum_{i=1}^{3} \epsilon' N'_{(11)i}$
$\sum_{i=1}^{2} \epsilon' N'_{(11)i}$
$\sum_{i=1}^{1} \epsilon' N'_{(11)i}$
15°
30°
45°
ϕ
0
15°
30°
45
ϕ
$\sum_{i=1}^{1} \epsilon' N'_{(22)i}$
$\sum_{i=1}^{2} \epsilon' N'_{(22)i}$
$\sum_{i=1}^{3} \epsilon' N'_{(22)i}$
Static $\epsilon' N'_{(22)}$
$\sum_{i=1}^{4} \epsilon' N'_{(22)i}$
1000
2000
$\epsilon' N'_{(22)}$

representation of the dynamic response. The superposed stress resultants at three meridional points are plotted as a function of time in Fig. 20.

CONCLUSION

The asymmetric response to free and forced vibrations of an initially-stressed membrane shell of revolution has been studied. Equations of motion have been presented for small free vibrations about a previously deformed middle surface. The assumptions inherent in the mathematical model are: 1) the thickness ratio is small compared to unity; 2) the moment resultants are negligible compared to the force resultants; 3) the material is elastic, homogeneous, and isotropic; and 4) the superimposed dynamic strains are infinitesimal.

The natural frequencies and mode shapes for the exact and the approximate formulations of the equations of motion were determined numerically using the generalized Holzer method. Convergence difficulties for steep shells were alleviated by suppressing extraneous solutions at intermediate points. In the neighborhood of the apex a special technique was used to integrate the equations of motion. This method is based on Taylor expansions of the displacements. For shells with rapidly varying geometries near the apex, it was found that more rapid convergence of the solutions was possible if Taylor expansions of functions of the displacements and of certain geometric quantities were used.

The modal method of analysis was used to determine the transient response of initially-stressed membrane shells to static and dynamic loads. The solution techniques developed for the free and forced response of the general shell of revolution were tested on several sample shell geometries with varied boundary conditions. It was found that the magnitude of the initial stress had a significant effect on the natural frequencies but did not significantly effect the associated mode shapes. Both the exact and approximate formulations yielded

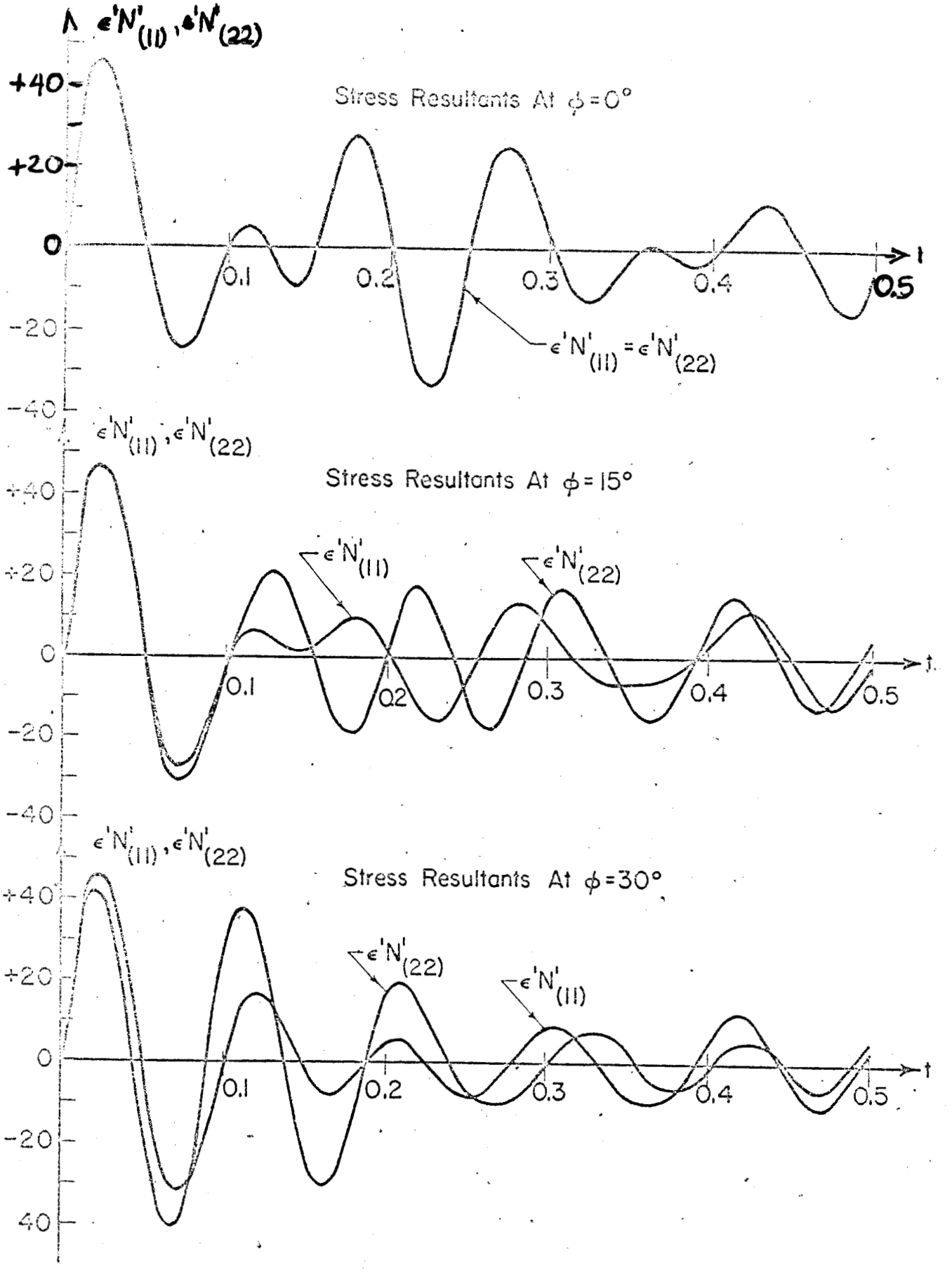
$\epsilon'N'_{(11)}, \epsilon'N'_{(22)}$
+40
+20
0
-20
-40
Stress Resultants At $\phi = 0°$
0.1
0.2
0.3
0.4
0.5
t
$\epsilon'N'_{(11)} = \epsilon'N'_{(22)}$
$\epsilon'N'_{(11)}, \epsilon'N'_{(22)}$
Stress Resultants At $\phi = 15°$
$\epsilon'N'_{(11)}$
$\epsilon'N'_{(22)}$
$\epsilon'N'_{(11)}, \epsilon'N'_{(22)}$
Stress Resultants At $\phi = 30°$
$\epsilon'N'_{(22)}$
$\epsilon'N'_{(11)}$

solutions in close agreement with each other.

Further research is needed on the determination of the dynamic response of isotropic and anisotropic shells with non-symmetric initial-stress states. The buckling behavior, local and global, of extremely thin initially-stressed shells is another important subject in need of study. For one type of initially-stressed shell, an inflatable shell, the determination of the local buckling characteristics is extremely important in that inflatables tend to wrinkle and kink at boundaries.

ACKNOWLEDGEMENTS

The results presented herein were derived as part of a research program of the Department of Civil Engineering at the University of Illinois, Urbana, Illinois relating to the study of Nonlinear Dynamic Analysis of Structures supported by a grant from the National Aeronautics and Space Administration (NGR-14-005-107).

The valuable assistance of Mr. Tzu-Cheng Chu, Research Assistant, Department of Civil Engineering, University of Illinois, in the checking of all equations, in the debugging of all computer programs, and in the preparation and execution of numerous sample problems is gratefully acknowledged. The cooperation of the University of Illinois in making their IBM 360 computer available for use is also acknowledged.

APPENDIX I. - REFERENCES

1. Biot, M.A., Mechanics of Incremental Deformation, John Wiley and Sons, Inc., N.Y., 1965.

2. Budiansky, B., "Notes on Non-Linear Shell Theory," Report SM - 14, Harvard University, Cambridge, Mass., July, 1967.

3. Carter, R.L., Robinson, A.R., and Schnobrich, W.C., "Free and Forced Vibrations of Hyperboloidal Shells of Revolution," Civil Engineering Studies, SRS No. 334, University of Illinois, Urbana, Illinois., Feb., 1968.

4. Cohen, G.A., "Computer Analysis of Asymmetric Free Vibrations of Ring-Stiffened Orthotropic Shells of Revolution," AIAA Journal, Vol. 3, No. 12, Dec., 1965, pp. 2305-2317.

5. Davenport, A.G., and Isyumov, N., "Dynamic and Static Action on Hyperbolic Cooling Tower Ia," University of Western Ontario, London, Canada, May, 1967.

6. Fernandez-Sintes, J. and Nachbar, W., "Rotationally Symmetric Problems of Highly Elastic Thin Membranes Subjected to Ring Loads," SUDAER No. 209, Stanford University, 1964.

7. Flugge, W., Stresses in Shells, Springer-Verlag, Berlin, 1960.

8. Goldberg, J.E., Setlur, A.V., and Alspaugh, D.W., "Computer Analysis of Non-Circular Cylindrical Shells," Symposium on Shell Structures, Int. Assoc. for Shell Structures, Budapest, Hungary, Sept. 1965.

9. Gol'denveizer, A.L., Theory of Elastic Thin Shells, Pergamon Press, 1961.

10. Green, A.E., and Adkins, J.E., Large Elastic Deformations, Oxford University Press, London, 1960.

11. Herrmann, G., and Shaw, J., "Vibrations of Thin Shells with Initial Stress," Journal of the Engineering Mechanics Division, ASCE, Vol. 91, No. 5, Oct., 1965.

12. Holzer, H., Die Berechnung der Drehscheingungen, Springer-Verlag, Berlin, 1921, Republished by J.W. Edwards, Publ., Inc., Ann Arbor, Mich., 1940.

13. Jacobson, L. S., and Ayre, R.S., Engineering Vibrations, McGraw-Hill Book Co., Inc., New York, 1958.

14. Kalnins, A., "On Vibrations of Elastic Spherical Shells," Journal of Applied Mechanics, ASME, Vol. 29, March, 1962, pp. 55-72.

15. Kalnins, A., "Free Vibrations of Rotationally Symmetric Shells," Journal of the Acoustical Society of America, Vol. 36, No. 7, July, 1964.

16. Koiter, W.T., "On the Nonlinear Theory of Thin Elastic Shells," Proc. Kon. Ned. Ak. Wet., Amsterdam, B69, pp. 1-54, 1966.

17. Kraus, H., and Kalnins, A., "Transient Vibration of Thin Elastic Shells," Journal of the Acoustical Society of America, Vol. 38, No. 6, Dec., 1965, pp. 994-1002.

18. Leonard, J.W., "Inflatable Shells: Pressurization Phase," Journal of the Eng. Mechanics Div., ASCE, Vol. 93, No. EM2, April 1967, pp. 207-227.

19. Leonard, J.W., "Inflatable Shells: In-Service Phase," Journal of the Engineering Mechanics Div., ASCE, Vol. 93, No. EM6, Dec. 1967, pp. 67-85.

20. Leonard, J.W., "Inflatable Shells: Non-symmetric In-Service Loads," Journal of the Engineering Mechanics Division, ASCE, Vol. 94, No. EM5, Oct., 1968, pp. 1231-1248.

21. Lestingi, J., "Nonsymmetric Buckling of Finitely Deformed Thin Elastic Shells of Revolution," Proc., ASCE Joint Specialty Conf. (EMD-STD), Optimization and Nonlinear Problems, April, 1968.

22. Liepins, A.A., "Free Vibrations of Prestressed Toroidal Membrane," AIAA Journal, Vol. 3, No. 10, Oct. 1965.

23. Mushtari, Kh.M. and Galinov, E.Z., "Nonlinear Theory of Thin Elastic Shells," Trans. publ. for NSF and NASA by The Israel Program for Scientific Translations, Chap. III, Jerusalem, 1961.

24. Naghdi, P.M., and Kalnins, A., "On Vibrations of Elastic, Spherical Shells," Journal of Applied Mechanics, ASME, Vol. 29, March 1962.

25. Newmark, N.N., "A Method of Computation for Structural Dynamics," Journal, Eng. Mechanics Div., ASCE, Vol. 85, No. EM 4, July, 1957.

26. Prasad, C., "On Vibrations of Spherical Shells," Journal, Acoustic Soc. of America, Vol. 36, 1964.

27. Ross, E.W., Jr., "Approximations in Nonsymmetric Shell Vibrations," AMRA TR 67-09, U.S. Army Materials Research Agency, Watertown, Mass., April, 1967.

28. Sanders, J.L., Jr., "Nonlinear Theories of Thin Shells," Quarterly of Applied Mechanics, Vol. XXI, No. 1, April 1968.

29. Simmonds, J.G., "The General Equations of Equilibrium of Rotationally Symmetric Membranes and Some Solutions for Uniform Centrifugal Loading," NASA TN D-816, 1961.

30. West., H.H., and Robinson, A.R., "A Re-examination of the Theory of Suspension Bridges," Civil Engineering Studies, SRS No. 322, University of Illinois, Urbana, Ill., June, 1967.

31. Zarghamee, M.S. and Robinson, A.R., "A Numerical Method for Analysis of Free Vibrations of Spherical Shells," AIAA Journal, Vol. 5, No. 7, July, 1967.

32. Zerna, W., "Elact Theory of Elastic Shells," Proc., World Conf. on Shell Structures, 1962.

APPENDIX II - NOTATION

$A_{\alpha\gamma} + \epsilon' A'_{\alpha\gamma}$ = metric tensor of M'

a = focal length of paraboloid, or distance defined by Fig. 13

a_m^n, b_m^n, c_m^n = Taylor series constants in Eqs. 13.

$B_{\alpha\gamma} + \epsilon' B'_{\alpha\gamma}$ = curvature tensor of M'

C, C_{cr} = coefficients of viscous damping

E = Young's modulus

F'^{γ}, F'^{3} = tensor components of the non-dimensional superposed load vector.

F_{ni} = mode participation factor

G = $LP_{(1)}\sqrt{A_{11}}/K$

$*h$ = one-half the thickness of initially-stressed shell

K = $2E\lambda L/(1-\nu^2)$

K_α = $N_{(\alpha\alpha)}/K$

L = smallest characteristic length of $*M$

$*M$ = middle surface of initially-stressed shell.

M' = middle surface of additionally deformed shell.

$N_{(\alpha\gamma)} + \epsilon' N'_{(\alpha\gamma)}$ = physical components of $n^{\alpha\gamma} + \epsilon' n'^{\alpha\gamma}$

$n^{\alpha\gamma} + \epsilon' n'^{\alpha\gamma}$ = force resultant tensor on M'

$*P$ = largest characteristic load on $*M$.

$P'_{(\alpha)}$, $P'_{(3)}$ = physical components of F'^{α}, F'^{3}

p = $\rho L^2(1-\nu^2)\,\omega^2/E$

$\bar{p}$ = internal pressure on $*M$

R = non-dimensional sphere radius

R_1, R_2 = non-dimensional radii of curvature of $*M$

r = perpendicular distance of a point on $*M$ from the axis of revolution.

t = time.

u'^{α}_{o}, u'^{3}_{o} = displacement functions defined by Eqs. 3.

u, v, w = displacement functions defined by Eqs. 6.

u^*, v^*, w^* = functions defined by Eqs. 9.

u^n, v^n, w^n = functions defined by Eqs. 10.

u^n_o, v^n_o, w^n_o = initial conditions on u^n, v^n, w^n, at $t = 0$.

V'^{α}_{o}, W' = tensor components of the non-dimensional superposed displacement vector.

$V'_{o(\alpha)}$, $V'_{o(3)}$ = physical components of V'_o, W.

x^{α} = non-dimensional coordinates of *M, $\alpha = 1, 2$.

β = C/C_{cr}.

$^*\Gamma^{\alpha}_{\rho\alpha} + \epsilon' \Gamma'^{\alpha}_{\rho\alpha}$ = Christoffel symbols of M'.

$\Delta\overline{P}$ = superposed load increment.

$\Delta\overline{V}$ = superposed initial displacement vector.

ϵ' = arbitrary small parameter defined by superposed loads.

θ = azimuth angle of a shell of revolution.

λ = thickness ratio = *h/L.

ν = Poisson's ratio.

ρ = mass density of initially-stressed shell.

φ = angle normal to *M makes with axis of revolution.

φ_o = one-half the opening angle of *M.

φ_1 = angular location of rigid plug.

ω = frequency.

Figure	Title
1	Shell of Revolution
2 (a,b,c)	Sphere Configurations
3	n = 0 Stress and Displacement Mode Shapes for a Sphere (Continuous, $\varphi_o = 45°$)
4	n = 1 Stress and Displacement Mode Shapes for a Sphere (Continuous, $\varphi_o = 45°$)
5	n = 2 Stress and Displacement Mode Shapes for a Sphere (Continuous, $\varphi_o = 45°$)
6	n = 0 Stress and Displacement Mode Shapes for a Sphere (Continuous, $\varphi_o = 90°$)
7	n = 1 Stress and Displacement Mode Shapes for a Sphere (Continuous, $\varphi_o = 90°$)
8	n = 2 Stress and Displacement Mode Shapes for a Sphere (Continuous, $\varphi_o = 90°$)
9	First Axisymmetric Mode Shapes for a Continuous Sphere Fixed at the Base
10	Effect of Initial Stress on Natural Frequencies of a Continuous Sphere
11	Mode Shapes for Spheres Fixed at Apex and With a Rigid Plug
12	Paraboloid Continuous at Apex and Fixed at Base
13	Toroid with a Rigid Plug Near Apex and Fixed at Apex
14	n = 0, 1 Mode Shapes for a Paraboloid Continuous at Apex and Fixed at $\varphi_o = 45°$
15	n = 0, 1, 2 Mode Shapes for a Toroid with a Rigid Plug at $\varphi = 30°$ and Fixed at 90°
16	Stress Resultants at $\varphi = 15°$, 35° of a Wind-Loaded Sphere Continuous at Apex and Fixed at $\varphi_o = 45°$
17	Comparisons of Static and Dynamic Results for a Wind-Loaded Sphere
18	Comparisons of Static and Dynamic Displacements for an Over-pressurized Sphere
19	Comparisons of Static and Dynamic Stresses for an Over-pressurized Sphere
20	Stresses at $\varphi = 0°$, 15°, 30° in a Continuous Sphere Fixed at $\varphi_o = 45°$ and Subjected to an Initial-Velocity Field.